Vglut2-based glutamatergic signaling in central noradrenergic neurons is dispensable for normal breathing and chemosensory reflexes

Author names and affiliations

Yuan Chang[1], Savannah Lusk[2], Russell Ray[1,2,3,4]

[1]Department of Molecular Physiology and Biophysics, Baylor College of Medicine, Houston TX

[2]Department of Neuroscience, Baylor College of Medicine, Houston TX

[3]McNair Medical Institute, Houston TX

[4]Corresponding author, russell.ray@bcm.edu

Abstract

Central noradrenergic (NA) neurons are key constituents of the respiratory homeostatic network. NA dysfunction is implicated in several developmental respiratory disorders including Central Congenital Hyperventilation Syndrome (CCHS), Sudden Infant Death Syndrome (SIDS) and Rett Syndrome. Multiple prior studies provide indirect evidence that glutamate is co-transmitted in subsets of NA neurons and may play a role in breathing control. If true, NA-glutamate co-transmission may also be mechanistically important in respiratory disorders. However, the extent of glutamate co-transmission in the central NA system remains uncharacterized and the requirement of NA derived glutamate in breathing has not been directly tested. Therefore, we fully characterized the cumulative fate maps and acute adult expression patterns of all three Vesicular Glutamate Transporters (Vglut1, Vglut2, and Vglut3) in NA neurons, identifying broad expression of Vglut2 as the dominant transporter in the NA system. Our functional studies showed that loss of Vglut2 throughout the NA system failed to alter breathing or metabolism under room air, hypercapnia, or hypoxia in unrestrained and conscious mice, which demonstrates that Vglut2-based glutamatergic signaling within the central NA system is not required for normal baseline breathing and hypercapnic, hypoxic chemosensory reflexes. It suggests that glutamate may be not a critical target to understand NA neuron dysfunction in respiratory diseases.

30 **Introduction**

31 Breathing is a vital and life-sustaining function supporting homeostatic processes, most critically
32 maintaining blood pH/CO_2 and O_2 levels within a narrow physiological range. Respiratory
33 homeostasis is mediated by neuron-modulated lung ventilation adjustments in response to
34 physiological deviations resulting in high pCO_2 or low pO_2 blood and tissue levels, known as the
35 hypercapnic and hypoxic reflexes respectively (Del Negro et al., 2018; Dick et al., 2018). These
36 reflexes are part of a complex brainstem neural network that integrates a multitude of
37 information streams across the central and peripheral nervous systems to regulate respiratory
38 output. Within this brainstem network, central noradrenergic (NA) neurons are known to be an
39 important component that plays a variety of roles in modulating breathing. Furthermore, NA
40 abnormalities have been implicated in several developmental disorders with respiratory and
41 chemosensory features such as Central Congenital Hyperventilation Syndrome (CCHS), Sudden
42 Infant Death Syndrome (SIDS) and Rett Syndrome (Beltrán-Castillo et al., 2017; Feldman et al.,
43 2013; Gauda et al., 2007; Viemari, 2008). Thus, understanding how central NA neurons modulate
44 respiratory chemoreflexes or chemosensory breathing is critically important for the development
45 of new diagnostic and therapeutic interventions to address respiratory pathophysiology.

46

47 Central noradrenergic neurons are commonly thought to exert their effect on breathing through
48 their primary neurotransmitter noradrenaline and adrenaline. Many *in vitro* experiments
49 suggested that noradrenaline is essential for development of normal respiratory rhythm of mice
50 and for modulation of respiratory chemoreflexes. For example, the blockade of α2 adrenergic
51 receptors and the activation of catecholamine biosynthesis significantly depresses and facilitates,
52 respectively, the respiratory rhythm generator, pre-Bötzinger complex (Zanella et al., 2006).
53 External noradrenaline application to RTN, a key central chemosensory center, altered activities
54 of subsets of RTN neurons. The blockade of α1 and α2 adrenergic receptors depressed and
55 enhanced noradrenaline-mediated RTN neuron activities respectively (Kuo et al., 2016).
56 Additionally, several respiratory disorders mentioned above showed various perturbations
57 across the noradrenergic system. The embryonic lethality of *Phox2b-/-* mice (a mouse model of
58 CCHS) can be (partially) rescued by maternal treatment with an α1 noradrenergic agonist. *Mecp2*

male mice (a mouse model of Rett Syndrome) show a reduction in noradrenaline levels and external application of noradrenaline can restore fictive eupneic breathing to control levels (Pattyn et al., 2000). Postmortem studies found abnormalities in noradrenaline levels in cases of SIDS in the locus coeruleus and medulla (Denoroy et al., 1987; Lavezzi et al., 2005; Obonai et al., 1998; Ozand and Tildon, 1983; Ozawa et al., 1999; Perrin et al., 1984) as well as loss of adrenergic receptors in the medulla (Chigr et al., 1989; Kopp et al., 1993; Mansouri et al., 2001; Ozawa et al., 2003; Takashima and Becker, 1991).

However, in addition to noradrenaline, several studies suggest that glutamate is co-transmitted in subsets of central NA neurons and therefore may also play a role in breathing control. Vesicular glutamate transporter 2 (Vglut2), a gene marker of glutamatergic signaling, has been shown to be co-expressed in subsets of central NA neurons including, C1/A1, C2/A2, A5, and LC in adult rats and mice (DePuy et al., 2013; Souza et al., 2022a; Stornetta et al., 2002a, 2002b; Yang et al., 2021), though NA specific expression of related Vglut1 and Vglut3 transporters remains unknown. Functionally, Abbott et al. (2014) showed that Vglut2 is required for an increase in respiratory rate when anterior C1 neurons are unilaterally opto-genetically stimulated. More circumstantially, Malheiros-Lima et al. (2020) showed that Vglut2-expressing C1 neurons project to the pFRG region, and hypoxic breathing was blunted after blockade of ionotropic glutamatergic receptors at the pFRG site in anesthetized rats, together supporting a role for anterior C1 neurons releasing glutamate at the pFRG site in turn to regulate breathing under hypoxia. Similarly, Malheiros-Lima et al. (2022) and Malheiros-Lima et al. (2018) showed that Vglut2-expressing C1 neurons project to the NA A5 region and the preBötzinger complex respectively, and again the blockade of ionotropic glutamatergic receptors at the A5 region or preBötzinger complex reduced the increase in phrenic nerve activities or in respiratory frequency elicited by optogenetic stimulation of C1 cells in an anesthetized preparation. Although these studies offer circumstantial evidence for NA-based Vglut2 signaling in respiratory control, it is not yet clear what the requirement is for NA-based glutamatergic signaling in homeostatic breathing in the awake and unrestrained animal and how that might inform upon disease.

87 To better understand the role of NA-based glutamatergic signaling in breathing, we first fully
88 characterized the recombinase-based cumulative fate maps for Vglut1, Vglut2 and Vglut3
89 expression and compared those maps to their real time expression profiles in central NA neurons
90 by RNA *in situ* hybridization in adult mice. We found that Vglut2 and Vglut3, previously
91 undescribed, both show co-expression in the adult central NA system. Secondly, to determine if
92 Vglut2-based glutamatergic signaling in NA neurons is required for respiratory homeostasis, we
93 conditionally ablated Vglut2 in all NA neurons and tested respiratory, chemosensory, and
94 metabolic function in unrestrained and conscious mice. Using the same genetic model in prior
95 studies, conditional deletion of Vglut2 in NA neurons did not significantly impact breathing under
96 room air, hypercapnic, or hypoxic conditions. These results suggest that NA Vglut2-based
97 glutamatergic signaling is dispensable for respiratory control and that glutamate may not be a
98 critical target to understand NA neuron dysfunction in respiratory diseases.
99
100 **Results**
101 **Cumulative fate maps of central noradrenergic neurons co-expressing Vglut1, Vglut2 and**
102 **Vglut3**
103 To fully characterize the expression profiles of all three glutamate markers Vglut1, Vglut2 and
104 Vglut3 in central noradrenergic neurons, we first used an intersectional genetic strategy (Figure
105 1A). We bred three Cre drivers *Vglut1-Cre/+, Vglut2-Cre/+ and Vglut3-Cre/+* to *DBH-p2a-Flpo/+*
106 (targeting noradrenergic neurons) mice respectively. The three compound lines of *Vglut1-Cre/+;*
107 *DBH-p2a-Flpo/+, Vglut2-Cre/+; DBH-p2a-Flpo/+, and Vglut3-Cre/+; DBH-p2a-Flpo/+* were then
108 crossed with the *RC::F_TdTomato_P_GFP (RC::FLTG)* intersectional reporter mice which express
109 tdTomato in cells co-expressing flippase (Flpo) while expressing eGFP in cells co-expressing both
110 Flpo and Cre recombinases. Thus, in each of the three intersectional reporter crosses, *Vglut1-*
111 *Cre/+; DBH-p2a-Flpo/+; RC::FLTG/+, Vglut2-Cre/+; DBH-p2a-Flpo/+; RC::FLTG/+ and Vglut3-Cre/+;*
112 *DBH-p2a-Flpo/+; RC::FLTG/+,* NA neurons co-expressing either Vglut1, Vglut2, or Vglut3 are
113 labeled by green fluorescent protein (eGFP) while NA neurons without any Vglut1/2/3 expression
114 are labelled by red fluorescent protein (tdTomato). By using this method, we characterized and
115 quantified the expression profiles of all three vesicular glutamate transporters Vglut1, Vglut2 and

116 Vglut3 across every NA nucleus in adult mice including A7, Locus Coeruleus (LC), sub CD/CV, A5,
117 anterior and posterior part of C1/A1, anterior and posterior part of C2/A2 (Figure 1B-D). *Vglut1-*
118 *Cre* was not co-expressed in any central NA nuclei in adult mice. However, *Vglut2-Cre* and *Vglut3-*
119 *Cre* both showed co-expression in central NA neurons. *Vglut3-Cre*-expressing NA neurons are
120 restricted to posterior C2/A2 and posterior C1/A1, and the majority is in posterior C2/A2 where
121 26.9 ± 3.16% NA neurons are *Vglut3-Cre*$^+$. In posterior C1/A1, only 1.26 ± 0.559% NA neurons are
122 *Vglut3-Cre*$^+$. Surprisingly, 84.6 ± 3.75% NA neurons in total have *Vglut2-Cre* co-expression and
123 each NA nucleus was predominantly labelled by *Vglut2-Cre* expression. The percentage of *Vglut2-*
124 *Cre*$^+$ NA neurons in A7, LC, A5, sub CD/CV, anterior and posterior part of C1/A1, anterior and
125 posterior part of C2/A2 is 69.8 ± 8.29%, 80.5 ± 3.78%, 84.8 ± 11.3%, 51.5 ± 2.61%, 99.0 ± 0.681%,
126 95.7 ± 2.40%, 96.1 ± 1.98%, 97.8 ± 0.771%, respectively (Mean ± SEM). The presence of *Vglut2-*
127 *Cre* co-expression in anterior NA groups was unexpected as previous *in situ* data in adult rats
128 found Vglut2$^+$ NA neurons only in the posterior NA populations C2/A2 and C1/A1 (DePuy et al.,
129 2013; Stornetta et al., 2002a, 2002b). Notably, however, the Vglut2 co-expression in the LC
130 region agrees with Yang et al. (2021) which also showed that a high percentage of LC NA neurons
131 are Vglut2$^+$ by using another intersectional strategy in mice, *TH-Flp; vGluT2-Cre; Ai65.* The
132 differences in our and other fate maps compared to *in situ* hybridization may either reflect early
133 gene expression that is down regulated in the adult or may reflect low levels of expression not
134 detectable by *in situ* hybridization but that are nonetheless sufficient to effect recombination in
135 the intersectional genetic strategy.
136
137 **Real time mRNA expression patterns of Vglut1, Vglut2 and Vglut3 in central noradrenergic**
138 **neurons in adult mice**
139 DePuy et al. (2013), Stornetta et al. (2002a) and Stornetta et al. (2002b) showed that Vglut2 co-
140 expression is only located in the C2/A2 and C1/A1 region in the adult rat without existing in
141 anterior NA nuclei in the brainstem by *in situ* hybridization. To verify if the real time NA-based
142 Vglut2 expression pattern in adult mice is the same as in adult rats and to further characterize
143 the expression patterns of the other two vesicular glutamate transporters (Vglut1 and Vglut3) in
144 adult mice, we performed fluorescent RNA *in situ* hybridization experiments. We co-stained

145 Vglut1, Vglut2, Vglut3 with DBH respectively in brain tissue of adult mice and characterized the
146 colocalization of Vglut1/2/3 with DBH in brainstem NA nuclei A7, LC, A5, sub CD/CV, anterior
147 C1/A1 and C2/A2, posterior C1/A1 and C2/A2 (Figure 2A-C). No Vglut1/DBH double positive
148 neurons were detected in any part of the central NA system, consistent with our fate map. Vglut3
149 mRNA colocalization with DBH is only found in the posterior part of C2/A2 and 27.1 ± 1.86% DBH^+
150 neurons have Vglut3 co-localization, again consistent with our fate map. For Vglut2, we only
151 found detectable levels of Vglut2 mRNA in C1/A1 and C2/A2 NA region, but not in A7, LC, A5, sub
152 CD/CV. Quantitatively, the percentage of Vglut2/DBH double positive neurons in anterior C1/A1,
153 anterior C2/A2, posterior C1/A1 and posterior C2/A2 is 84.7 ± 5.82%, 66.3 ± 0.335%, 35.7 ± 3.01%
154 and 90.1 ± 2.45%, respectively. This result is consistent with the previous *in situ* data in adult rats
155 (DePuy et al., 2013; Stornetta et al., 2002a, 2002b) suggesting that there is no obvious
156 expression difference of Vglut2 in the central NA system between mouse and rat. However, the
157 Vglut2 *in situ* data did not show expression in anterior NA populations. This difference between
158 our *in situ* data and fate map data supports our previous hypothesis that many NA neurons
159 expressed Vglut2 at some point from early development toward adulthood but the expression of
160 Vglut2 is turned back down during adulthood. Interestingly, Yang et al. (2021) did show adult
161 Vglut2 co-expression in LC by a viral injection of both Cre and Flpo-dependent eYFP into the LC
162 of a bi-transgenic mouse with both TH-Flpo and Vglut2-Cre. To verify this result, we injected an
163 AAV virus containing Cre-dependent tdTomato (pAAV-EF1a-DIO-tdTomato-WPRE) into the LC
164 region of adult *Vglut2-Cre* mice. With TH co-staining in LC, our result is consistent with Yang et
165 al. (2021) (Figure 2 supplement 1). Additionally, Souza et al. (2022a) showed about 28.5% A5
166 neurons are Vglut2 $mRNA^+$ in adult rats by RNA scope, a method which is more sensitive than the
167 traditional *in situ* hybridization we used here. These data suggest that some adult NA neurons in
168 LC and A5 have Vglut2 co-expression, but the Vglut2 mRNA level cannot be detected by
169 traditional *in situ* hybridization.
170
171 **Vglut2 expression is effectively knocked down in the whole central noradrenergic system in**
172 ***TgDBH-Cre/+; Vglut2$^{flox/flox}$* mice**

173 To investigate the requirement of Vglut2-based glutamatergic signaling in the central NA system
174 in breathing under physiological challenges, we used *TgDBH-Cre/+; Vglut2*$^{flox/flox}$ as the mouse
175 model which is the same model used by Abbott et al. (2014) to show that *Vglut2* expression in
176 the NA system was required for a modest increase in respiratory frequency following unilateral
177 optogenetic stimulation of anterior C1. To verify if Vglut2 expression is effectively removed from
178 central NA neurons in *TgDBH-Cre/+; Vglut2*$^{flox/flox}$ mice, we carried out fluorescent RNA *in situ*
179 hybridization for Vglut2 and DBH in the mouse brainstems and compared the Vglut2 signal
180 intensity in DBH^{+} neurons in *TgDBH-Cre/+; Vglut2*$^{flox/flox}$ and its littermate controls. We found that
181 Vglut2 mRNA expression is 96.4 $\pm$ 0.226% decreased compared to controls, indicating that the
182 Vglut2 is effectively recombined to abrogate expression in NA neurons (Figure 3A-B).
183
184 **Vglut2-based glutamatergic signaling in central NA neurons is not required for baseline**
185 **breathing nor for the hypercapnic ventilatory reflex under distinct CO_2 challenges**
186 Multiple prior studies provide indirect evidence that NA glutamate transmission may play roles
187 in respiratory function, particularly that anterior C1 neurons mediate the hypoxic ventilatory
188 response through the pFRG/RTN and/or the NA A5 group (Malheiros-Lima et al., 2022, 2020).
189 Additionally, the A5 group has been implicated in the hypercapnic reflex (Haxhiu et al., 1996).
190 Thus, we sought to determine if Vglut2-based glutamatergic signaling in central NA neurons is
191 necessary to regulate baseline breathing and the hypercapnic chemoreflex in awake and
192 unrestrained animals. We used whole-body barometric plethysmography to measure the
193 breathing and metabolism of conscious and free-moving mice. After a five-day habituation
194 protocol, the ventilation response of *TgDBH-Cre/+; Vglut2*$^{flox/flox}$ mice and their littermate
195 controls was measured under room air and hypercapnia (5% CO_2) (Figure 4A). Surprisingly,
196 *TgDBH-Cre/+; Vglut2*$^{flox/flox}$ mice didn't show significant differences in overall respiratory output
197 (V_E/V_{O2}), respiratory rate (V_f), tidal volume (V_T), minute ventilation (V_E) and metabolism demand
198 (V_{O2}) compared to their littermate controls under both room air and 5% CO_2 challenge (Figure 4B
199 and Table 1-2). These results suggested that Vglut2-based glutamatergic signaling is not required
200 for regulating baseline breathing and hypercapnic ventilatory reflex under 5% CO_2.
201

202 To further investigate if Vglut2-based glutamatergic signaling in central NA neurons is required
203 for ventilation response of higher CO_2 challenges, we also measured the breathing of *TgDBH-*
204 *Cre/+; Vglut2$^{flox/flox}$* mice under 7% CO_2 and 10% CO_2. We found that under the 7% CO_2 condition,
205 *TgDBH-Cre/+; Vglut2$^{flox/flox}$* mice showed only a significantly decreased tidal volume (V_T), but the
206 overall respiratory output (V_E/V_{O2}), respiratory rate (V_f), minute ventilation (V_E) and metabolism
207 demand (V_{O2}) didn't show a significant difference between the mutant mice and their sibling
208 controls (Figure 5A-B and Table 3). This result suggests that Vglut2-based glutamatergic signaling
209 in central NA neurons is not required or at least is not as important as previously expected for
210 regulating the hypercapnic ventilatory reflex under 7% CO_2.
211
212 Under 10% CO_2 challenge, none of the overall respiratory outputs (V_E/V_{O2}), respiratory rate (V_f),
213 tidal volume (V_T), minute ventilation (V_E) and metabolism demand (V_{O2}) were significantly
214 different between *TgDBH-Cre/+; Vglut2$^{flox/flox}$* mice and their littermate controls, suggesting that
215 Vglut2-based glutamatergic signaling in central NA neurons is not required for the hypercapnic
216 ventilatory reflex under 10% CO_2 (Figure 6A-B and Table 4).
217
218 **Vglut2-based glutamatergic signaling in central NA neurons is not required for the hypoxic**
219 **ventilatory reflex under 10% O_2**
220 To determine if Vglut2-based glutamatergic signaling in central NA neurons is necessary to
221 regulate the hypoxic chemoreflex, we measured the ventilation response of *TgDBH-Cre/+;*
222 *Vglut2$^{flox/flox}$* mice under 10% O_2. We analyzed the five respiratory parameters in three 5-min time
223 periods under 10% O2 challenge. No significant difference was found in the overall respiratory
224 output (V_E/V_{O2}), respiratory rate (V_f), tidal volume (V_T), minute ventilation (V_E) and metabolism
225 demand (V_{O2}) between *TgDBH-Cre/+; Vglut2$^{flox/flox}$* mice and controls in either of the three 5-min
226 10% O_2 period (Figure 7A-B and Table 5). These data suggest that Vglut2-based glutamatergic
227 signaling in central NA neurons is not required for the hypoxic ventilatory reflex under 10% O_2.
228
229 **Discussion**

230 Neuron co-transmission of two or more neurotransmitters across excitatory, inhibitory, and
231 neuro-modulatory facets is becoming an increasingly appreciated phenomenon in the central
232 nervous system. Functional interrogation of co-transmission is essential not only to understand
233 the distinct and cooperative roles that multiple signaling molecules may play at the synapse but
234 also to determine the most critical targets for potential therapeutics. It has long been appreciated
235 that central NA neurons co-express Vesicular glutamate transporter 2 (Vglut2), the major
236 glutamate marker among three glutamate transporters (DePuy et al., 2013; Souza et al., 2022a;
237 Stornetta et al., 2002a, 2002b; Yang et al., 2021). Given the expression of Vglut2, it has been
238 assumed that the central NA neurons co-produce, release, and functionally communicate with
239 post-synaptic neurons via glutamate (Abbott et al., 2014, 2012; DePuy et al., 2013; Guyenet and
240 Stornetta, 2021; Guyenet et al., 2013; Holloway et al., 2013; Malheiros-Lima et al., 2022, 2020,
241 2018; Yang et al., 2021). However, to our knowledge, the potential for the central NA neurons to
242 express other glutamate transporters Vglut1 or Vglut3 has not been reported. To determine if
243 central NA neurons express either Vglut1 or Vglut3 and to confirm the Vglut2 expression, we
244 carried out cumulative intersectional fate mapping using *Vglut1-Cre/+; DBH-p2a-Flpo/+;*
245 *RC::FLTG/+, Vglut2-Cre/+; DBH-p2a-Flpo/+; RC::FLTG/+ and Vglut3-Cre/+; DBH-p2a-Flpo/+;*
246 *RC::FLTG/+* compound mouse lines. As this approach maps the cumulative history of expression,
247 we also examined acute adult expression of Vglut1, Vglut2 and Vglut3 using fluorescent RNA *in*
248 *situ* hybridization. Our *in situ* results for Vglut2 agreed with earlier published outcomes (DePuy
249 et al., 2013; Stornetta et al., 2002a, 2002b) showing as much as 80% expression in posterior NA
250 neurons. However, there was no appreciable signal in anterior groups (A7, LC, A5, sub CD/CV).
251 This lack of expression was in stark contrast to the cumulative fate map for Vglut2, showing as
252 much as 75% of the anterior central NA neurons were recombined by the *Vglut2-Cre* over the
253 lifetime of the animal. To further interrogate the acute activity of the *Vglut2-Cre* in the Locus
254 Coeruleus in the adult mouse, we injected a Cre responsive virus in LC of *Vglut2-Cre* mice. Here
255 we observed about 20% of the cells recombined. The outcomes from the cumulative fate map
256 and acute injections are in agreement with published results from Yang et al. (2021). Notably our
257 use of the *DBH-p2a-Flpo* avoided expression in the PBN that was seen in the *TH-Flp* mouse. In
258 addition, 28.5% A5 neurons were shown to be Vglut2^{+} in adult rats by RNA scope (Souza et al.,

259 2022b). It is notable that both our lab and work published by (DePuy et al., 2013; Stornetta et al.,
260 2002a, 2002b) failed to detect Vglut2 expression in anterior groups, but that apparently very low
261 levels can be detected by more sensitive recombinase and RNA scope methods. Additional
262 electrophysiological evidence suggests that this expression is functional (Yang et al., 2021). Our
263 data suggests that Vglut2 co-expression in anterior NA groups is time dependent, though the
264 underlying temporal dynamics of Vglut2 remain unknown. It is notable that we see nearly 80%
265 of the LC and 85% of A5 recombined in the intersectional strategy representing lifetime
266 expression, but our and other studies find only 20% of the LC and 28.5% of A5 may be expressing
267 Vglut2 at any given moment in adults. This suggests either a temporal restriction in expression
268 as the animal matures or may reflect dynamic change driven by behavioral or physiological
269 experiences.
270
271 For Vglut1, neither fate map nor *in situ* hybridization revealed any co-expression within the
272 central NA system. However, Vglut3 expression was found in the posterior part of NA neurons
273 including C2/A2 and C1/A1, which is first characterized by this study. The majority of this Vglut3
274 co-expression is restricted to the posterior part of the C2/A2 NA population. This NA region has
275 not been heavily implicated in respiratory control nonetheless it readily lends itself to
276 interrogation by intersectional genetic methods and *in situ* hybridization. Given its distal
277 expression from anterior C1, it is unlikely that Vglut3 would compensate for loss of Vglut2 in
278 anterior C1, though this has not been ruled out. Further, while Vglut3 is a marker of glutamatergic
279 neurons, its role in neurotransmission is not wholly defined as Vglut3 is typically found in soma
280 and dendrites (Fremeau et al., 2004).
281
282 Based on the Vglut2 co-expression in NA neurons, several studies suggest that glutamate in NA
283 populations has a functional role in breathing control. Those studies provide a mix of
284 circumstantial, indirect, or limited evidence for the potential role of Vglut2-based glutamatergic
285 signaling in central NA neurons in breathing regulation. It has not yet been shown whether or not
286 NA-based Vglut2 signaling is required for respiratory control due to experimental caveats or
287 limitations.

288 Abbott et al. (2014) showed that conditionally knocking out Vglut2 in the whole central NA
289 system attenuated a modest increase in respiratory rate resulting from unilateral C1 optogenetic
290 stimulation. Absolute values and other respiratory parameters, including tidal volume (V_T) and
291 minute ventilation (V_E) were not reported, making direct comparison difficult. While the
292 optogenetic stimulation did drive a Vglut2 dependent increase in respiratory rate, it is not clear
293 if the resulting change in breathing reflects a native feature of the network that might be engaged
294 in chemosensory responses, exercise, or volitional control. Thus, it remains possible that strong
295 optogenetic stimulation of a small, isolated population drives a Vglut2 dependent but ectopic
296 function that is not typically engaged in the normal operation of the breathing network. Such
297 ectopic outcomes could come from several potential, non-exclusive mechanisms. First, unilateral
298 stimulation could drive a network hysteresis or dysregulation akin to a focal injury that is not a
299 typical biological feature (Ducros et al., 2003). This point is well made in Abbott et al. (2013) in
300 their discussion of C1 optogenetic stimulation where they state, "resulting cardiorespiratory
301 response pattern should not be considered strictly "physiological," because a physiological
302 response is never initiated by selective activation of a single cluster of CNS neurons and the
303 various subsets of C1 neurons are presumably never recruited en bloc under any physiological
304 condition". Second, strong stimulation could result in overwhelming synaptic mechanisms (i.e.,
305 glial uptake) resulting in glutamate spillover and unintended cross talk to affect extra-synaptic
306 neurons proximal to targeted NA fibers. Activity dependent spillover transmission has been
307 documented elsewhere in the nervous system (Henneberger et al., 2020; Hülsmann et al., 2000).
308 Third, the outcomes could be secondary to a different autonomic or behavioral function requiring
309 NA-derived glutamatergic signaling involving metabolism or circulation (DePuy et al., 2013; Yang
310 et al., 2021).
311
312 More circumstantially, Malheiros-Lima et al. (2020) suggested C1 neurons potentially release
313 glutamate at the pFRG site to regulate breathing under hypoxia by providing three indirect lines
314 of evidence: 1) Vglut2-expressing C1 neurons project to the pFRG region; 2) Increased breathing
315 was blunted after blockade of ionotropic glutamatergic receptors at the pFRG site under
316 anesthesia using chemical hypoxia; 3) Depletion of C1 neurons eliminated the increased

317 breathing elicited by hypoxia. However, 1) the glutamatergic signaling targeting the pFRG region
318 is not necessarily from C1 NA neurons since glutamatergic neurons from other regions also
319 project to the pFRG site (Yang and Feldman, 2018).Thus, it is possible that the glutamatergic
320 signaling that is required for hypoxic response is derived from other glutamatergic neurons such
321 as the pre-Bötzinger complex and the RTN itself; 2) C1 neuron depletion knocks out all the
322 signaling modalities in the C1 population including both noradrenaline and glutamate. It is not
323 clear which signaling drives the hypoxic response.
324
325 Similarly, Malheiros-Lima et al. (2022) and Malheiros-Lima et al. (2018) showed that Vglut2-
326 expressing C1 neurons project to the NA A5 region and the preBötzinger complex respectively.
327 The blockade of ionotropic glutamatergic receptors at the A5 region or preBötzinger complex
328 reduced the increase in phrenic nerve activities or the breathing frequency caused by
329 optogenetic stimulation of C1 cells in anesthetized preparation. Together these results suggest
330 that Vglut2-expressing C1 neurons communicate with A5 or preBötzinger complex neurons by
331 releasing glutamate in turn to regulate phrenic nerve activities or breathing frequency. Again,
332 these two studies showed that C1 neurons are important to regulate phrenic nerve activities or
333 breathing frequency, however, it is not necessarily through a direct C1-A5 or C1-preBötzinger
334 complex glutamatergic pathway, whereas an indirect multi-synaptic pathway originating with C1
335 noradrenaline and ending with glutamate transmission from an intermediate to A5 or
336 preBötzinger complex cannot be ruled out. Importantly, in all four studies noted here, respiratory
337 measurements were limited or proxies of breathing under anesthesia were used. The role of NA-
338 Vglut2 signaling was not reported in the context of an awake, unrestrained animal under
339 normoxic, hypoxic, or hypercapnic breathing.
340
341 Thus, the limitations and indirect lines of the evidence in these studies raised the question as to
342 whether or not glutamatergic signaling in central NA neurons is required or necessary to
343 modulate respiratory homeostasis under more physiologically relevant circumstances and if NA-
344 derived glutamate is an important mechanism to understand the pathophysiology of NA neurons
345 in respiratory diseases. The goal of our study was to test the requirement of NA-based

346 glutamatergic signaling in breathing homeostasis in the awake and unrestrained animal under
347 conditions that would engage the whole respiratory control network rather than a singular
348 component that may drive hysteresis or artifactual outcomes. Our *in vivo* breathing data under
349 room air, hypoxic, and multiple hypercapnic conditions failed to show the requirement of NA-
350 derived Vglut2 in normal breathing and respiratory chemoreflexes directly. To ensure a rigorous
351 and robust conclusion, first we use exactly the same mouse model, *TgDBH-Cre/+; Vglut2*$^{flox/flox}$,
352 as Abbott et al. (2014) used, and confirmed, by a second method (fluorescent RNA *in situ*
353 hybridization) that Vglut2 expression was indeed abrogated in the whole central NA system. Our
354 results are in strong agreement with DePuy et al. (2013) that recombination is efficient. Notably,
355 we assayed for expression at the cell body, rather than the fibers and see no singular cell body
356 that is scored positive. Second, we measured the breathing of conscious, unrestrained, and
357 habituated mice under physiological challenges including normoxia, hypercapnia and hypoxia.
358 Third, multiple respiratory and metabolic parameters were measured and reported in absolute
359 values including respiratory rate, tidal volume, minute ventilation, oxygen consumption, overall
360 respiratory output (minute ventilation normalized to oxygen consumption) in order to visualize
361 breathing function comprehensively. Fourth, our experimental design was overpowered (i.e.,
362 n=16-21 vs 5-13 needed for power based on power analysis and n=7-8 reported in other
363 manuscripts). Each respiratory/metabolic parameter for each physiological condition including
364 room air, hypercapnia, and hypoxia was derived by quantifying the entire respiratory trace and
365 analyzed between mutant and sibling controls by using a powerful linear mixed-effects
366 regression model with animal type (experimental vs. control) as fixed effects, animal ID as a
367 random effect and including sex as a variable (there was no sex specific effect) (Lusk et al., 2022)..
368
369 Despite our experimental design and the extensive nature of our measurements, there remain
370 several considerations in the interpretation of our data. First, we uncovered a novel NA co-
371 expressed glutamate transporter, Vglut3. It remains a formal possibility that Vglut3 somehow
372 compensates for the loss of Vglut2, however we argue that this is unlikely for the following
373 reasons. First, our model is the same used in the other study where an effect was seen with
374 optogenetic stimulation. Second, focus has been on anterior C1 whereas Vglut3 is expressed in

375 the posterior CA domains. Another consideration is that pre- or post-natal developmental
376 compensation corrects for the loss of NA derived glutamate. Again, we argue that is not likely, as
377 we are using the same adult model that provided the most direct evidence and first functionally
378 demonstrated a potential role for C1-derived glutamate in breathing. Second, Abbott et al.
379 (2014) highlight that Vglut2 negative NA neurons showed no obvious abnormalities in number,
380 morphology, and projection patterns. Third, we have examined the requirement of NA-expressed
381 Vglut2 in P7 neonate mice in the auto-resuscitation reflex and saw no differences (data not
382 shown). However, this could be better tested by using the *TgDBH-CreER* (Stubbusch et al., 2011)
383 to more acutely remove Vglut2 expression (though this leaves a window of 2-3 weeks for
384 compensation to occur). Yet another consideration in interpreting our results is that we only
385 address the loss of NA-Vglut2 based signaling across the entire NA system. It remains a formal
386 possibility that we have removed Vglut2 dependent signaling from two counter balancing regions
387 of the NA system and are therefore left with null results whereas removal from anterior C1 alone
388 would show a requirement. To test this possibility, it would require an intersection conditional
389 approach, something that has not yet been shown to be efficient and effective and would be
390 beyond the scope of these studies. Additionally, in our studies, we account for potential
391 metabolic changes that may underlie or be coordinate with changes in breathing. However, in
392 this study we did not test for potential changes in blood pressure or other autonomic functions
393 as well as affective state that may, in some obscure way, compensate for changes in breathing.
394 Lastly, our results are loss of function in nature. We do not test sufficiency or gain of function and
395 cannot fully rule out a role for NA-Vglut2 based glutamatergic signaling in the control of
396 breathing.
397
398 From a translational perspective, our data questions whether or not glutamatergic signaling in
399 NA neurons is likely to be a key mechanism and therefore a therapeutic target for breathing
400 disorders, such as Rett syndrome and SIDS. *Mecp2*-deficient mice (a mouse model of Rett
401 Syndrome that phenocopies many human symptoms) showed both a deficiency of NA
402 populations (reduced number of NA neurons in C2/A2 and C1/A1 group) and highly variable
403 respiratory rhythm at around 4-5 weeks of age (Roux et al., 2007; Viemari et al., 2005). 80% Rett

404 Syndrome patients experience breathing issues, such as unstable breathing, episodes of
405 hyperventilation and breathing holds, during the whole lifespan including both childhood and
406 adulthood (Ramirez et al., 2020). SIDS decedents show NA abnormalities and are hypothesized
407 to ultimately succumb from a failure in cardiorespiratory autoresuscitation (Chigr et al., 1989;
408 Garcia et al., 2013; Kopp et al., 1993; Mansouri et al., 2001; Ozawa et al., 2003; Takashima and
409 Becker, 1991). However, *TgDBH-Cre/+; Vglut2*$^{flox/flox}$ mice, have normal baseline and
410 chemosensory respiratory parameters as adults and neonate mice show normal
411 autoresuscitation indicating that perturbed NA based glutamatergic signaling may not be a key
412 driver in these or other related respiratory pathophysiologies.
413
414 In conclusion, our studies demonstrated the extent of glutamate as a functional vesicular
415 glutamate transporter co-expression in central noradrenergic system. We were able to
416 characterize a novel Vglut3-expressing NA population in the posterior C2/A2 nuclei and found a
417 different Vglut2 co-expression pattern in anterior NA groups from a cumulative intersectional
418 fate map compared to a viral fate map and *in situ* hybridization in the adult, suggesting that
419 anterior NA populations may have a time-dependent or experience-dependent manner for
420 Vglut2 expression. Furthermore, despite prior studies providing indirect and circumstantial
421 evidence that noradrenergic-based glutamatergic signaling may play a role in control of
422 breathing, our studies that remove Vglut2 expression from noradrenergic neurons failed to
423 perturb room air breathing, the hypercapnic ventilatory reflex, and the hypoxic ventilatory reflex,
424 providing further insight into the potential role of NA-glutamate transmission in the control of
425 breathing. Based on our data, we suggest that noradrenergic-based glutamatergic signaling is not
426 required for regulating baseline breathing or the hypercapnic and hypoxic respiratory
427 chemoreflexes, and glutamate may not be a critical mechanistic component of NA neuron
428 dysfunction in respiratory disorders.
429
430 **Materials and Methods**
431 **Ethical Approval**

432 Studies were approved by the Baylor College of Medicine Institutional Animal Care and Use
433 Committee (IACUC) under protocol AN-6171, and all experiments reported here were performed
434 in accordance with relevant guidelines and regulations.
435
436 **Breeding, Genetic Background, and Maintenance of Mice**
437 We maintained all our heterozygous mouse strains by backcrossing to wildtype C57BL/6J mice
438 and homozygous mouse strains by sibling crosses. For immunofluorescence experiments,
439 heterozygous *Vglut1*-Cre *(Jax Stock No: 023527), Vglut2-Cre (Jax Stock No: 016963) and Vglut3-*
440 *Cre (Jax Stock No: 018147)* were mated with heterozygous *DBH-p2a-Flpo (MMRRC ID: 41575)*
441 (Sun and Ray, 2016) mice respectively to derive compound lines with both Cre and Flpo alleles
442 (*Vglut1-Cre/+; DBH-p2a-Flpo/+, Vglut2-Cre/+; DBH-p2a-Flpo/+, and Vglut3-Cre/+; DBH-p2a-*
443 *Flpo/+*). Then these three compound lines were each mated with homozygous
444 *RC::F_TdTomato_P_GFP (RC::FLTG, Jax Stock No: 026932)* to derive three different intersectional
445 mouse lines *Vglut1/Cre/+; DBH-p2a-Flpo/+; RC::FLTG/+, Vglut2/Cre/+; DBH-p2a-Flpo/+;*
446 *RC::FLTG/+ and Vglut3/Cre/+; DBH-p2a-Flpo/+; RC::FLTG/+.* For *in situ* hybridization experiments,
447 wildtype C57BL/6J mice were ordered from the Center of Comparative Medicine (CCM), Baylor
448 College of Medicine. For NA-Vglut2 conditional loss of function *in situ* hybridization and
449 plethysmography experiments, hemizygous *TgDBH-Cre (MMRRC ID: 036778-UCD GENSAT)* mice
450 were mated with homozygous *Vglut2$^{flox/flox}$ (Jax Stock No: 012898)* to derive *TgDBH-Cre;*
451 *Vglut2$^{flox/+}$*. *TgDBH-Cre; Vglut2$^{flox/+}$* mice were mated with *Vglut2$^{flox/flox}$* to derive *TgDBH-Cre;*
452 *Vglut2$^{flox/flox}$*. Sibling mice that lacked the Cre allele or carried the Cre allele but lacked the floxed
453 Vglut2 alleles were used as controls. Rosa26 specific primers for the *RC::FLTG* mice were 5'-
454 GCACTTGCTCTCCCAAAGTC, 5'-GGGCGTACTTGGCATATGAT, and 5'-CTTTAAGCCTGCCCAGAAGA
455 (Ray et al., 2011) and yield a 495 bp band (targeted) and 330 bp band (wt). Cre-specific primers
456 for all Cre drivers were 5'-ATCGCCATCTTCCAGCAGGCGCACCATTGCCC and 5'-
457 GCATTTCTGGGGATTGCTTA and yielded a 550 bp band if positive. Flpo-specific primers for *DBH-*
458 *p2a-Flpo* are 5'- CACGCCCAGGTACTTGTTCT and 5'-CCACAGCAAGAAGATGCTGA (Sun and Ray,
459 2016) and yielded a 226 bp band if positive. Vglut2^{flox} specific primers for Vglut2-floxed mice are
460 available at The Jackson Laboratory website (https://www.jax.org/strain/012898).

461 **Immunofluorescence staining**

462 *Vglut1, Vglut2, or Vglut3-Cre/+; DBH-p2a-Flpo/+; RC::FLTG/+* adult mice were sacrificed and
463 transcardially perfused with 0.1 M phosphate-buffered saline (PBS) then with 4%
464 paraformaldehyde (PFA) in PBS. Mouse brains were dissected out and fixed for 2h in 4% PFA
465 before a PBS rinse and dehydration in 30% sucrose in PBS. Brains were embedded in OCT blocks,
466 sectioned at the thickness of 30µm, mounted on slides, and stored at -80°C until they were ready
467 for staining. The slides were hydrated in 0.1% Triton-X in PBS (PBST) for 15 mins, blocked with 5%
468 donkey serum in 0.1% PBST for 1h at room temperature and then incubated with primary
469 antibodies for 72 hours at 4°C in 0.1% PBST with 5% donkey serum. Tissues were washed in 0.1%
470 PBST 3 times for 10 min each and then incubated with secondary antibodies for 2hs at room
471 temperature in 0.1% PBST with 5% donkey serum. Slides were washed with 0.1% PBST for 10 min
472 and washed in PBS twice for 10 min each, stained for DAPI, washed 3 times for 10 min each with
473 PBS and mounted in ProLong Glass (Invitrogen). The following primary and secondary antibodies
474 were used: chicken anti-GFP (1:1,000, Abcam ab13970), rabbit anti-dsRed (1:1,000, Clontech
475 632496), donkey anti-chicken Cy2 (1:500, Jackson 703-225-155), donkey anti-rabbit Cy3 (1:500,
476 Jackson 711-165-152).

477

478 **In situ hybridization**

479 Mouse brains were dissected out from adult mice with 6-8 week of age, sectioned into
480 25µm brain sections and mounted on slides. We generated a digoxigenin (DIG)-labeled
481 mRNA antisense probe against *Vglut1, Vglut2, and Vglut3* and fluorescein (FITC)-labeled mRNA
482 against *DBH* using reverse-transcribed mouse cDNA as a template and an RNA DIG or FITC-
483 labeling kits from Roche (Sigma). Primer and probe sequences for the *Vglut1, Vglut2, Vglut3 and*
484 *DBH* probes are available in the Allen Brain Atlas (http://www.brain-map.org). For the Vglut2 and
485 DBH double ISH in *TgDBH-Cre/+; Vglut2*$^{flox/flox}$ and their littermate controls, we generated a new
486 Vglut2 probe targeting exon 2 of Vglut2 specifically (Tong et al., 2007) and the probe sequence is
487 892-1144bp as Slc17a6 transcript variant 1 and the size is 253bp. ISH was performed by the
488 RNA In Situ Hybridization Core at Baylor College of Medicine using an automated robotic
489 platform as previously described (Yaylaoglu et al., 2005) with modifications of the protocol for

490 double ISH. Modifications in brief (see Yaylaoglu et al. (2005) for buffer descriptions): both
491 probes were hybridized to the tissue simultaneously. After the described washes and blocking
492 steps the DIG-labeled probes were visualized using tyramide-Cy3 Plus (1/75 dilution, 15-minute
493 incubation, Akoya Biosciences). After washes in TNT, the remaining HRP-activity was quenched
494 by a 10-minute incubation in 0.2M HCl. The sections were then washed in TNT, blocked in TNB
495 for 15 minutes, and incubated at room temperature for 30 minutes with HRP-labeled sheep anti-
496 FITC antibody (1/500 in TNB, Roche/Sigma). Following washes in TNT, the FITC-labeled probe was
497 visualized using tyramide-FITC Plus (1/50 dilution, 15-minute incubation, Akoya Biosciences).
498 Following washes in TNT, the slides were stained with DAPI (invitrogen), washed again, removed
499 from the machine, and mounted in ProLong Diamond (Invitrogen).
500
501 **Viral Injection**
502 To verify Vglut2 co-expression in LC in adult mice (Yang et al., 2021), 6-week-old *Vglut2-Cre* mice
503 were injected with pAAV-EF1a-DIO-tdTomato-WPRE virus (RRID:Addgene_133786, obtained
504 from Joshua Ortiz at the Optogenetics and Viral Vectors Core at the Jan and Dan Duncan
505 Neurological Research Institute, 1ul at 7.90E+10 Gc/mL) into the LC (coordinates from bregma
506 anteroposterior −5.4 mm, lateral + 0.8 mm and dorsoventral – 4.0 mm) and allowed to incubate
507 for 4 weeks.
508
509 **Plethysmography**
510 Plethysmography on conscious and free-moving mice was carried out as described in (Ray et al.,
511 2011) on 6-8-week-old adult animals with at least 16 animals in both the experimental and
512 control group for each experiment. Animals were subjected to a five-day habituation protocol
513 with each day including several minutes of handling, temperature taken by rectal probe and at
514 least 30 min exposure in the plethysmography chamber (Martinez et al., 2019). Plethysmography
515 was then performed for each mouse within 1 week of the last day of habituation. On the day of
516 testing, mice were taken out from their home cage, weighed, and rectal temperature was taken.
517 Animals were then placed into a flow-through, temperature-controlled (about 32°C with real-
518 time temperature recording) plethysmography chamber and allowed to acclimate for at least 45

519 min in room air (21% O_2/79% N_2) conditions. After acclimation and measurement under room
520 air, the chamber gas was switched to a hypercapnic or hypoxic mixture of 5% CO_2/21% O_2/74%
521 N_2, 7% CO_2/21% O_2/72% N_2, 10% CO_2/21% O_2/69% N_2, or 10% O_2/90% N_2, depending on the
522 protocol, for 20 min. Chamber gas was then switched back to room air for another 20 min. The
523 animals were removed from the chamber and rectal temperature was measured immediately
524 after the mice were taken out from the chamber.
525
526 **Plethysmography data analysis and statistics**
527 Details were previously described in (Martinez et al., 2019; Ray et al., 2011). Plethysmography
528 pressure changes were measured using a Validyne DP45 differential pressure transducer, CD15
529 carrier demodulator and a reference chamber, and were recorded with LabChart Pro in real time.
530 Respiratory waveforms were analyzed by the BASSPRO module of the Breathe Easy software to
531 determine respiratory frequency (V_f), tidal volume (V_T), minute ventilation (V_E), oxygen
532 consumption (V_{O2}) and ventilatory equivalents for oxygen (V_E/V_{O2}) (Lusk et al., 2022). A power
533 analysis was performed using the reported effect size in Abbott et al. (2014) which used the same
534 mouse model as we used here and 5-13 mice were necessary to observe a statistically significant
535 result (Abbott et al. (2014) was able to see a significant difference between two groups with n=7
536 mice). In our experiments, the sample size for each group (*TgDBH-Cre/+; Vglut2*$^{flox/flox}$ and
537 control) exceeded 13. Results (V_f, V_E, V_T, V_{O2}, V_E/V_{O2}) for room air and hypercapnic or hypoxic
538 data were compared between *TgDBH-Cre/+; Vglut2*$^{flox/flox}$ cohorts and sibling controls using a
539 linear mixed-effects regression model with animal type (experimental vs. control) as fixed effects
540 and animal ID as a random effect (Lusk et al., 2022). A $p < 0.05$ was used to indicate statistical
541 significance, and individual data points, mean, and standard error of the mean are shown on all
542 charts. The graphs were plotted by Prism 8.
543
544 **Image quantification**
545 Images were taken by using a Zeiss upright epifluorescent microscope and a Zeiss LSM 880 with
546 Airyscan FAST confocal microscope. Images were captured using Zen software with z-stack
547 function from top to bottom with 0.34µm intervals, exported, and then analyzed in Imaris using

548 the spots and surface functions. For quantification of immunofluorescence staining, each GFP$^+$
549 area coincident with DAPI (to denote nuclear localization) was defined as Vglut2 or Vglut3-
550 expressing NA neurons while each tdTomato$^+$ area coincident with DAPI was defined as NA
551 neurons without any Vglut2 or Vglut3 co-expression. For quantification of Vglut2 or Vglut3 with
552 DBH double *in situ* hybridization in adult WT mice, DBH$^+$ areas coinciding with DAPI were
553 identified as NA neurons and the DBH$^+$ areas overlapped with Vglut2/3$^+$ pixels and DAPI were
554 defined as NA neurons colocalized with Vglut2/3. The number of Vglut2/3$^+$ NA neurons and
555 Vglut2/3$^-$ NA neurons was counted in each image for both immunofluorescence and in situ
556 experiments and the percentage of Vglut2/3$^+$ NA neurons among all NA neurons in each NA
557 nucleus in each mouse brainstem was calculated every other brain section unilaterally. For
558 quantification of Vglut2 and DBH double ISH in *TgDBH-Cre/+; Vglut2$^{flox/flox}$* and their littermate
559 controls, Vglut2 pixel intensities in DBH$^+$ areas coincident with DAPI (NA neurons) were measured
560 in mutant and control images separately. The Vglut2 pixel intensity in NA neurons of control
561 brains was normalized as 1 and the relative Vglut2 pixel intensity of NA neurons in mutant brains
562 compared to that in control brains was calculated. At least three mouse brains were examined
563 for each set of experiments in each group. All quantitative results were graphed using Prism 8.
564
565 **Data availability**
566 All the data supporting this study is available from the corresponding author upon request.
567
568 **Acknowledgments**
569 We thank the Optical Imaging & Vital Microscopy Core (OiVM) at Baylor College of Medicine with
570 the expert assistance of Jason Kirk for confocal imaging. We thank BCM Neuropathology Core
571 and Tao Lin for tissue sectioning. We thank the RNA In Situ Hybridization Core at Baylor College
572 of Medicine with the expert assistance of Cecilia Ljungberg for performing in situ hybridization
573 (NIH S10 OD016167 and NIH IDDRC Grant P50 HD103555). We thank Dr. Joshua Ortiz and Dr.
574 Benjamin Arenkiel at the NRI Optogenetics and Viral Vectors Core for providing Cre-responsive
575 AAV virus used in viral injection.
576

577 **Author contributions**

578 YC designed and completed immunofluorescence staining, imaging, and plethysmography
579 experiments, analyzed data, and prepared the manuscript.

580 SL completed the viral injection experiments.

581 RR conceptualized and designed the study, analyzed the data, and prepared the manuscript.

582

583 **Competing interests**

584 No competing interests are declared.

585

586 **Figure 1. Cumulative fate maps of glutamate co-expressing NA neurons characterized by**
587 **intersectional genetics.** (A) Breeding schematic. *Vglut1-Cre/+*, *Vglut2-Cre/+* and *Vglut3-Cre/+*
588 were each bred with *DBH-p2a-Flpo/+* mice respectively. These *Vglut1, Vglut2, or Vglut3-Cre/+;*
589 *DBH-p2a-Flpo/+* compound lines were then crossed with the *RC::F_TdTomato_P_GFP*
590 intersectional reporter mice (*RC::FLTG*). In each of the three intersectional reporter crosses, NA
591 neurons co-expressing either Vglut1, Vglut2, or Vglut3 are labeled by green fluorescent protein
592 (eGFP) while NA neurons without any Vglut1,2, or 3 expression are labelled by red fluorescent
593 protein (tdTomato). Shown as an example is the *Vglut2-Cre/+; DBH-p2a-Flpo/+ RC::FLTG*
594 intersectional reporter line. (B) Quantification of the percentage of Vglut2-coexpressing NA
595 neurons among NA neurons in each brainstem NA nuclei including A7, LC, A5, sub CD/CV, anterior
596 C1/A1 and C2/A2, posterior C1/A1 and C2/A2. (C) Quantification of the percentage of Vglut3-
597 coexpressing NA neurons among NA neurons in each NA nuclei. (D) Fluorescent expression of
598 tdTomato (red) and eGFP (green) in coronal sections of Vglut1, Vglut2, or Vglut3 intersectional
599 reporter lines in brainstem NA nuclei. Nucleus is labeled by DAPI (blue). Scale bar 50µm.

600

601 **Figure 2. Characterization of real time co-expression of Vglut1, Vglut2 and Vglut3 in brainstem**
602 **NA neurons in adult mice by fluorescent *in situ* hybridization.** (A) Representative images of
603 Vglut1, Vglut2, or Vglut3 and DBH double ISH in coronal sections of WT mice in all of brainstem
604 NA nuclei in adult mice. DBH (green), Vglut1/2/3 (red), DAPI (cyan). Scale bar 50µm. (B)

605 Quantification of the percentage of Vglut2 co-expression in NA neurons in each NA nuclei. (C)
606 Quantification of the percentage of Vglut3 co-expression in NA neurons in each NA nuclei.
607
608 **Figure 3. DBH with Vglut2 co-staining by fluorescent *in situ* hybridization confirms that Vglut2**
609 **expression is disrupted in the whole central NA system in *TgDBH-Cre/+; Vglut2$^{flox/flox}$* mice.** (A)
610 Representative images of Vglut2 and DBH double ISH in anterior C1/A1, posterior C1/A1, anterior
611 C2/A2 and posterior C2/A2 in control and *TgDBH-Cre/+; Vglut2$^{flox/flox}$* mice. DBH (green), Vglut2
612 (red), DAPI (cyan). Scale bar 20µm.(B) Quantification of intensity of Vglut2 signal in control and
613 *TgDBH-Cre/+; Vglut2$^{flox/flox}$* mice.
614
615 **Figure 4. Vglut2 conditional knockout in central noradrenergic neurons fails to alter baseline**
616 **breathing and the hypercapnic ventilatory reflex (5% CO_2).** (A) Mouse model schematic and
617 experimental protocol including habituation and hypercapnia protocol. (B) Under both room air
618 and hypercapnia (5% CO_2), *TgDBH-Cre/+; Vglut2$^{flox/flox}$* mice didn't show significant changes in
619 respiratory output (V_E/V_{O2}), minute ventilation (V_E), respiratory rate (V_f), tidal volume (V_T), and
620 metabolism demand (V_{O2}). Linear mixed-effects regression model, *p<0.05.
621
622 **Figure 5. Vglut2 conditional knockout in central noradrenergic neurons fails to alter the**
623 **majority of hypercapnic ventilation parameters and metabolism under 7% CO_2.** (A) Mouse
624 model schematic and experimental protocol including habituation and hypercapnia protocol. (B)
625 Knocking out Vglut2 in the whole NA system failed to alter ventilation (V_E/V_{O2}, V_f, V_E) and
626 metabolism (V_{O2}) but only showed a significantly reduce in V_T under 7% CO_2 condition. Linear
627 mixed-effects regression model, *p<0.05.
628
629 **Figure 6. Vglut2 conditional knockout in central noradrenergic neurons fails to alter the**
630 **hypercapnic ventilatory reflex (10% CO_2).** (A) Mouse model schematic and experimental
631 protocol including habituation and hypercapnia protocol. (B) Knocking out Vglut2 in the whole
632 NA system didn't significantly alter ventilation (V_E/V_{O2}, V_f, V_T, V_E) and metabolism (V_{O2}) under 10%
633 CO_2 condition. Linear mixed-effects regression model, *p<0.05.

634 **Figure 7. Vglut2 conditional knockout in central noradrenergic neurons fails to alter the hypoxic**
635 **ventilatory reflex (10% O_2).** (A) Mouse model schematic and experimental protocol including
636 habituation and hypoxia protocol. (B) Knocking out Vglut2 in the whole NA system didn't show
637 significant breathing changes including V_E/V_{O2}, V_E, V_f, V_T, and V_{O2} in either of the three five-minute
638 time periods under hypoxia (10% O_2). Linear mixed-effects regression model, *p<0.05.
639
640 **Figure 2 Supplement 1. Virus injection of Cre-dependent tdTomato into LC of *Vglut2-Cre* mice.**

641 **Table 1.** Respiratory and metabolic values under room air conditions and the statistical tests.

642 **Table 2.** Respiratory and metabolic values under 5% CO_2 conditions and the statistical tests.

643 **Table 3.** Respiratory and metabolic values under 7% CO_2 conditions and the statistical tests.

644 **Table 4.** Respiratory and metabolic values under 10% CO_2 conditions and the statistical tests.

645 **Table 5.** Respiratory and metabolic values under 10% O_2 conditions and the statistical tests.

646
647 **References**

648 Abbott SB, Kanbar R, Bochorishvili G, Coates MB, Stornetta RL, Guyenet PG. 2012. C1 neurons
649 excite locus coeruleus and A5 noradrenergic neurons along with sympathetic outflow in rats.
650 *J Physiol (Lond)* **590**:2897–2915. doi:10.1113/jphysiol.2012.232157
651 Abbott SBG, DePuy SD, Nguyen T, Coates MB, Stornetta RL, Guyenet PG. 2013. Selective
652 optogenetic activation of rostral ventrolateral medullary catecholaminergic neurons
653 produces cardiorespiratory stimulation in conscious mice. *J Neurosci* **33**:3164–3177.
654 doi:10.1523/JNEUROSCI.1046-12.2013
655 Abbott SBG, Holloway BB, Viar KE, Guyenet PG. 2014. Vesicular glutamate transporter 2 is
656 required for the respiratory and parasympathetic activation produced by optogenetic
657 stimulation of catecholaminergic neurons in the rostral ventrolateral medulla of mice in vivo.
658 *Eur J Neurosci* **39**:98–106. doi:10.1111/ejn.12421
659 Beltrán-Castillo S, Olivares MJ, Contreras RA, Zúñiga G, Llona I, von Bernhardi R, Eugenín JL.
660 2017. D-serine released by astrocytes in brainstem regulates breathing response to CO2
661 levels. *Nat Commun* **8**:838. doi:10.1038/s41467-017-00960-3
662 Chigr F, Najimi M, Jordan D, Denoroy L, Pearson J, Tommasi M, Gilly R, Kopp N. 1989.
663 [Immunohistochemical absence of adrenergic neurons in the dorsal part of the solitary tract
664 nucleus in sudden infant death]. *C R Acad Sci III, Sci Vie* **309**:543–549.
665 Del Negro CA, Funk GD, Feldman JL. 2018. Breathing matters. *Nat Rev Neurosci* **19**:351–367.
666 doi:10.1038/s41583-018-0003-6
667 Denoroy L, Gay N, Gilly R, Tayot J, Pasquier B, Kopp N. 1987. Catecholamine synthesizing
668 enzyme activity in brainstem areas from victims of sudden infant death syndrome.
669 *Neuropediatrics* **18**:187–190. doi:10.1055/s-2008-1052477

670 DePuy SD, Stornetta RL, Bochorishvili G, Deisseroth K, Witten I, Coates M, Guyenet PG. 2013.
671 Glutamatergic neurotransmission between the C1 neurons and the parasympathetic
672 preganglionic neurons of the dorsal motor nucleus of the vagus. *J Neurosci* **33**:1486–1497.
673 doi:10.1523/JNEUROSCI.4269-12.2013
674 Dick TE, Dutschmann M, Feldman JL, Fong AY, Hülsmann S, Morris KM, Ramirez JM, Smith JC,
675 Respiratory Neurobiology Consortium. 2018. Facts and challenges in respiratory
676 neurobiology. *Respir Physiol Neurobiol* **258**:104–107. doi:10.1016/j.resp.2015.01.014
677 Ducros L, Vahedi K, Similowski T, Bousser M-G, Payen D. 2003. Uncontrollable high-frequency
678 tachypnea in a case of unilateral medial medullary infarct. *Intensive Care Med* **29**:841–844.
679 doi:10.1007/s00134-003-1658-6
680 Feldman JL, Del Negro CA, Gray PA. 2013. Understanding the rhythm of breathing: so near, yet
681 so far. *Annu Rev Physiol* **75**:423–452. doi:10.1146/annurev-physiol-040510-130049
682 Fremeau RT, Voglmaier S, Seal RP, Edwards RH. 2004. VGLUTs define subsets of excitatory
683 neurons and suggest novel roles for glutamate. *Trends Neurosci* **27**:98–103.
684 doi:10.1016/j.tins.2003.11.005
685 Garcia AJ, Koschnitzky JE, Ramirez J-M. 2013. The physiological determinants of sudden infant
686 death syndrome. *Respir Physiol Neurobiol* **189**:288–300. doi:10.1016/j.resp.2013.05.032
687 Gauda EB, Cristofalo E, Nunez J. 2007. Peripheral arterial chemoreceptors and sudden infant
688 death syndrome. *Respir Physiol Neurobiol* **157**:162–170. doi:10.1016/j.resp.2007.02.016
689 Guyenet PG, Stornetta RL, Bochorishvili G, Depuy SD, Burke PGR, Abbott SBG. 2013. C1
690 neurons: the body's EMTs. *Am J Physiol Regul Integr Comp Physiol* **305**:R187-204.
691 doi:10.1152/ajpregu.00054.2013
692 Guyenet PG, Stornetta RL. 2021. Rostral ventrolateral medulla, retropontine region and
693 autonomic regulations. *Auton Neurosci* **237**:102922. doi:10.1016/j.autneu.2021.102922
694 Haxhiu MA, Yung K, Erokwu B, Cherniack NS. 1996. CO2-induced c-fos expression in the CNS
695 catecholaminergic neurons. *Respir Physiol* **105**:35–45. doi:10.1016/0034-5687(96)00034-5
696 Henneberger C, Bard L, Panatier A, Reynolds JP, Kopach O, Medvedev NI, Minge D, Herde MK,
697 Anders S, Kraev I, Heller JP, Rama S, Zheng K, Jensen TP, Sanchez-Romero I, Jackson CJ,
698 Janovjak H, Ottersen OP, Nagelhus EA, Oliet SHR, Stewart MG, Nägerl UV, Rusakov DA. 2020.
699 LTP induction boosts glutamate spillover by driving withdrawal of perisynaptic astroglia.
700 *Neuron* **108**:919-936.e11. doi:10.1016/j.neuron.2020.08.030
701 Holloway BB, Stornetta RL, Bochorishvili G, Erisir A, Viar KE, Guyenet PG. 2013. Monosynaptic
702 glutamatergic activation of locus coeruleus and other lower brainstem noradrenergic
703 neurons by the C1 cells in mice. *J Neurosci* **33**:18792–18805. doi:10.1523/JNEUROSCI.2916-
704 13.2013
705 Hülsmann S, Oku Y, Zhang W, Richter DW. 2000. Metabotropic glutamate receptors and
706 blockade of glial Krebs cycle depress glycinergic synaptic currents of mouse hypoglossal
707 motoneurons. *Eur J Neurosci* **12**:239–246.
708 Kopp N, Chigr F, Denoroy L, Gilly R, Jordan D. 1993. Absence of adrenergic neurons in nucleus
709 tractus solitarius in sudden infant death syndrome. *Neuropediatrics* **24**:25–29. doi:10.1055/s-
710 2008-1071508
711 Kuo F-S, Falquetto B, Chen D, Oliveira LM, Takakura AC, Mulkey DK. 2016. In vitro
712 characterization of noradrenergic modulation of chemosensitive neurons in the
713 retrotrapezoid nucleus. *J Neurophysiol* **116**:1024–1035. doi:10.1152/jn.00022.2016

714 Lavezzi AM, Ottaviani G, Mingrone R, Matturri L. 2005. Analysis of the human locus coeruleus in
715 perinatal and infant sudden unexplained deaths. Possible role of the cigarette smoking in the
716 development of this nucleus. *Brain Res Dev Brain Res* **154**:71–80.
717 doi:10.1016/j.devbrainres.2004.10.007
718 Lusk S, Ward CS, Chang A, Twitchell-Heyne A, Fattig S, Allen G, Jankowsky J, Ray R. 2022.
719 Breathe Easy, an automated respiratory data pipeline for waveform characteristic analysis.
720 *BioRxiv*. doi:10.1101/2022.12.02.518741
721 Malheiros-Lima MR, Silva JN, Souza FC, Takakura AC, Moreira TS. 2020. C1 neurons are part of
722 the circuitry that recruits active expiration in response to the activation of peripheral
723 chemoreceptors. *eLife* **9**. doi:10.7554/eLife.52572
724 Malheiros-Lima MR, Silva TM, Takakura AC, Moreira TS. 2022. A5 noradrenergic-projecting C1
725 neurons activate sympathetic and breathing outputs in anaesthetized rats. *Exp Physiol*
726 **107**:147–160. doi:10.1113/EP089691
727 Malheiros-Lima MR, Totola LT, Lana MVG, Strauss BE, Takakura AC, Moreira TS. 2018. Breathing
728 responses produced by optogenetic stimulation of adrenergic C1 neurons are dependent on
729 the connection with preBötzinger complex in rats. *Pflugers Arch* **470**:1659–1672.
730 doi:10.1007/s00424-018-2186-0
731 Mansouri J, Panigrahy A, Filiano JJ, Sleeper LA, St John WM, Kinney HC. 2001. Alpha2 receptor
732 binding in the medulla oblongata in the sudden infant death syndrome. *J Neuropathol Exp*
733 *Neurol* **60**:141–146.
734 Martinez VK, Saldana-Morales F, Sun JJ, Zhu PJ, Costa-Mattioli M, Ray RS. 2019. Off-Target
735 Effects of Clozapine-N-Oxide on the Chemosensory Reflex Are Masked by High Stress Levels.
736 *Front Physiol* **10**:521. doi:10.3389/fphys.2019.00521
737 Obonai T, Yasuhara M, Nakamura T, Takashima S. 1998. Catecholamine neurons alteration in
738 the brainstem of sudden infant death syndrome victims. *Pediatrics* **101**:285–288.
739 doi:10.1542/peds.101.2.285
740 Ozand PT, Tildon JT. 1983. Alterations of catecholamine enzymes in several brain regions of
741 victims of sudden infant death syndrome. *Life Sci* **32**:1765–1770. doi:10.1016/0024-
742 3205(83)90840-8
743 Ozawa Y, Obonai T, Itoh M, Aoki Y, Funayama M, Takashima S. 1999. Catecholaminergic
744 neurons in the diencephalon and basal ganglia of SIDS. *Pediatr Neurol* **21**:471–475.
745 doi:10.1016/s0887-8994(99)00033-8
746 Ozawa Y, Takashima S, Tada H. 2003. Alpha2-adrenergic receptor subtype alterations in the
747 brainstem in the sudden infant death syndrome. *Early Hum Dev* **75 Suppl**:S129-38.
748 doi:10.1016/j.earlhumdev.2003.08.016
749 Pattyn A, Goridis C, Brunet JF. 2000. Specification of the central noradrenergic phenotype by
750 the homeobox gene Phox2b. *Mol Cell Neurosci* **15**:235–243. doi:10.1006/mcne.1999.0826
751 Perrin DG, Cutz E, Becker LE, Bryan AC, Madapallimatum A, Sole MJ. 1984. Sudden infant death
752 syndrome: increased carotid-body dopamine and noradrenaline content. *Lancet* **2**:535–537.
753 doi:10.1016/s0140-6736(84)90763-3
754 Ramirez J-M, Karlen-Amarante M, Wang J-DJ, Bush NE, Carroll MS, Weese-Mayer DE, Huff A.
755 2020. The pathophysiology of rett syndrome with a focus on breathing dysfunctions.
756 *Physiology (Bethesda)* **35**:375–390. doi:10.1152/physiol.00008.2020

757 Ray RS, Corcoran AE, Brust RD, Kim JC, Richerson GB, Nattie E, Dymecki SM. 2011. Impaired
758 respiratory and body temperature control upon acute serotonergic neuron inhibition. *Science*
759 **333**:637–642. doi:10.1126/science.1205295
760 Roux J-C, Dura E, Moncla A, Mancini J, Villard L. 2007. Treatment with desipramine improves
761 breathing and survival in a mouse model for Rett syndrome. *Eur J Neurosci* **25**:1915–1922.
762 doi:10.1111/j.1460-9568.2007.05466.x
763 Souza GMPR, Stornetta DS, Vitali AJ, Wildner H, Zeilhofer HU, Campbell JN, Abbott SBG. 2022a.
764 Chemogenetic activation of noradrenergic A5 neurons increases blood pressure and visceral
765 sympathetic activity in adult rats. *Am J Physiol Regul Integr Comp Physiol* **323**:R512–R531.
766 doi:10.1152/ajpregu.00119.2022
767 Souza GMPR, Stornetta RL, Stornetta DS, Guyenet PG, Abbott SBG. 2022b. Adrenergic C1
768 neurons monitor arterial blood pressure and determine the sympathetic response to
769 hemorrhage. *Cell Rep* **38**:110480. doi:10.1016/j.celrep.2022.110480
770 Stornetta RL, Sevigny CP, Guyenet PG. 2002a. Vesicular glutamate transporter DNPI/VGLUT2
771 mRNA is present in C1 and several other groups of brainstem catecholaminergic neurons. *J*
772 *Comp Neurol* **444**:191–206. doi:10.1002/cne.10141
773 Stornetta RL, Sevigny CP, Schreihofer AM, Rosin DL, Guyenet PG. 2002b. Vesicular glutamate
774 transporter DNPI/VGLUT2 is expressed by both C1 adrenergic and nonaminergic
775 presympathetic vasomotor neurons of the rat medulla. *J Comp Neurol* **444**:207–220.
776 doi:10.1002/cne.10142
777 Stubbusch J, Majdazari A, Schmidt M, Schütz G, Deller T, Rohrer H. 2011. Generation of the
778 tamoxifen-inducible DBH-Cre transgenic mouse line DBH-CT. *Genesis* **49**:935–941.
779 doi:10.1002/dvg.20773
780 Sun JJ, Ray R. 2016. Generation of Two Noradrenergic-Specific Dopamine-Beta-Hydroxylase-
781 FLPo Knock-In Mice Using CRISPR/Cas9-Mediated Targeting in Embryonic Stem Cells. *PLoS*
782 *ONE* **11**:e0159474. doi:10.1371/journal.pone.0159474
783 Takashima S, Becker LE. 1991. Delayed dendritic development of catecholaminergic neurons in
784 the ventrolateral medulla of children who died of sudden infant death syndrome.
785 *Neuropediatrics* **22**:97–99. doi:10.1055/s-2008-1071424
786 Tong Q, Ye C, McCrimmon RJ, Dhillon H, Choi B, Kramer MD, Yu J, Yang Z, Christiansen LM, Lee
787 CE, Choi CS, Zigman JM, Shulman GI, Sherwin RS, Elmquist JK, Lowell BB. 2007. Synaptic
788 glutamate release by ventromedial hypothalamic neurons is part of the neurocircuitry that
789 prevents hypoglycemia. *Cell Metab* **5**:383–393. doi:10.1016/j.cmet.2007.04.001
790 Viemari J-C, Roux J-C, Tryba AK, Saywell V, Burnet H, Peña F, Zanella S, Bévengut M,
791 Barthelemy-Requin M, Herzing LBK, Moncla A, Mancini J, Ramirez J-M, Villard L, Hilaire G.
792 2005. Mecp2 deficiency disrupts norepinephrine and respiratory systems in mice. *J Neurosci*
793 **25**:11521–11530. doi:10.1523/JNEUROSCI.4373-05.2005
794 Viemari J-C. 2008. Noradrenergic modulation of the respiratory neural network. *Respir Physiol*
795 *Neurobiol* **164**:123–130. doi:10.1016/j.resp.2008.06.016
796 Yang B, Sanches-Padilla J, Kondapalli J, Morison SL, Delpire E, Awatramani R, Surmeier DJ. 2021.
797 Locus coeruleus anchors a trisynaptic circuit controlling fear-induced suppression of feeding.
798 *Neuron* **109**:823-838.e6. doi:10.1016/j.neuron.2020.12.023
799 Yang CF, Feldman JL. 2018. Efferent projections of excitatory and inhibitory preBötzinger
800 Complex neurons. *J Comp Neurol* **526**:1389–1402. doi:10.1002/cne.24415

801 Yaylaoglu MB, Titmus A, Visel A, Alvarez-Bolado G, Thaller C, Eichele G. 2005. Comprehensive
802 expression atlas of fibroblast growth factors and their receptors generated by a novel robotic
803 in situ hybridization platform. *Dev Dyn* **234**:371–386. doi:10.1002/dvdy.20441
804 Zanella S, Roux JC, Viemari JC, Hilaire G. 2006. Possible modulation of the mouse respiratory
805 rhythm generator by A1/C1 neurones. *Respir Physiol Neurobiol* **153**:126–138.
806 doi:10.1016/j.resp.2005.09.009

Figure 1

A

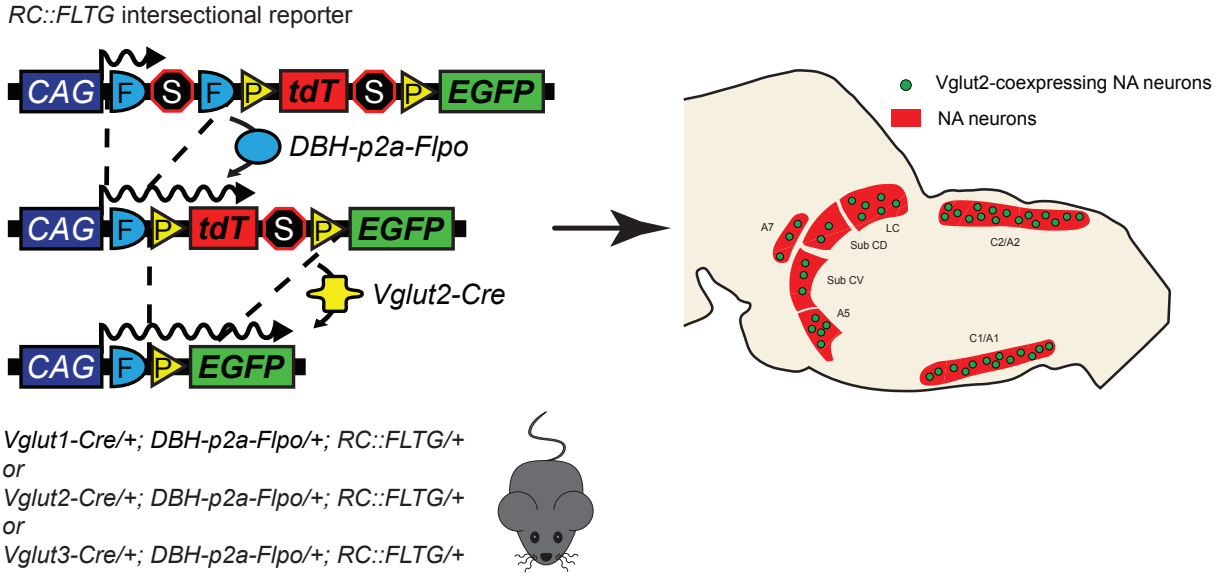
RC::FLTG intersectional reporter
CAG
F
S
F
P
tdT
S
P
EGFP
DBH-p2a-Flpo
CAG
F
P
tdT
S
P
EGFP
Vglut2-Cre
CAG
F
P
EGFP
Vglut2-coexpressing NA neurons
NA neurons
A7
LC
Sub CD
C2/A2
Sub CV
A5
C1/A1
Vglut1-Cre/+; DBH-p2a-Flpo/+; RC::FLTG/+
or
Vglut2-Cre/+; DBH-p2a-Flpo/+; RC::FLTG/+
or
Vglut3-Cre/+; DBH-p2a-Flpo/+; RC::FLTG/+

B

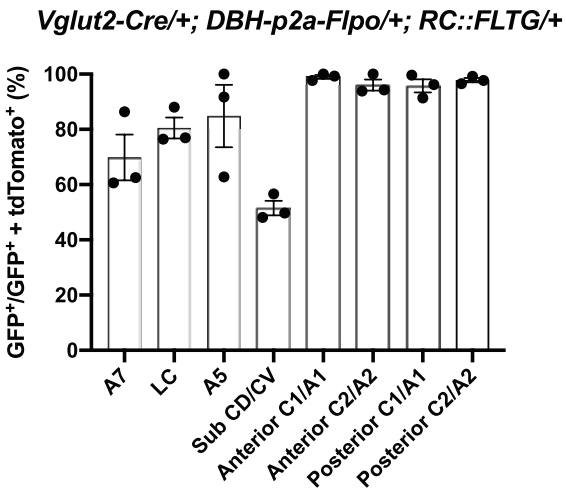
Vglut2-Cre/+; DBH-p2a-Flpo/+; RC::FLTG/+
GFP+/GFP+ + tdTomato+ (%)
100
80
60
40
20
0
A7
LC
A5
Sub CD/CV
Anterior C1/A1
Anterior C2/A2
Posterior C1/A1
Posterior C2/A2

C

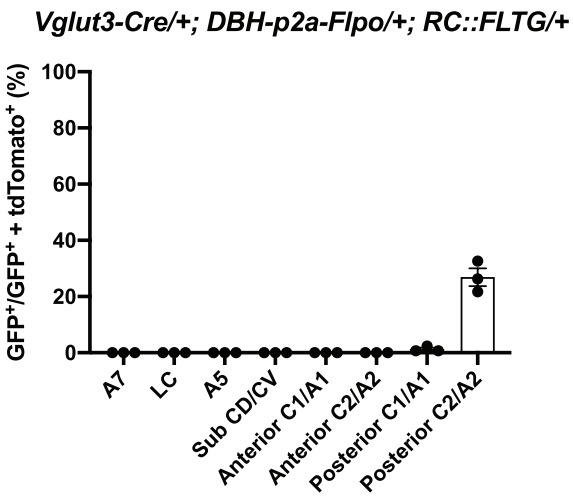
Vglut3-Cre/+; DBH-p2a-Flpo/+; RC::FLTG/+
GFP+/GFP+ + tdTomato+ (%)
100
80
60
40
20
0
A7
LC
A5
Sub CD/CV
Anterior C1/A1
Anterior C2/A2
Posterior C1/A1
Posterior C2/A2

Figure 1. cont.

D

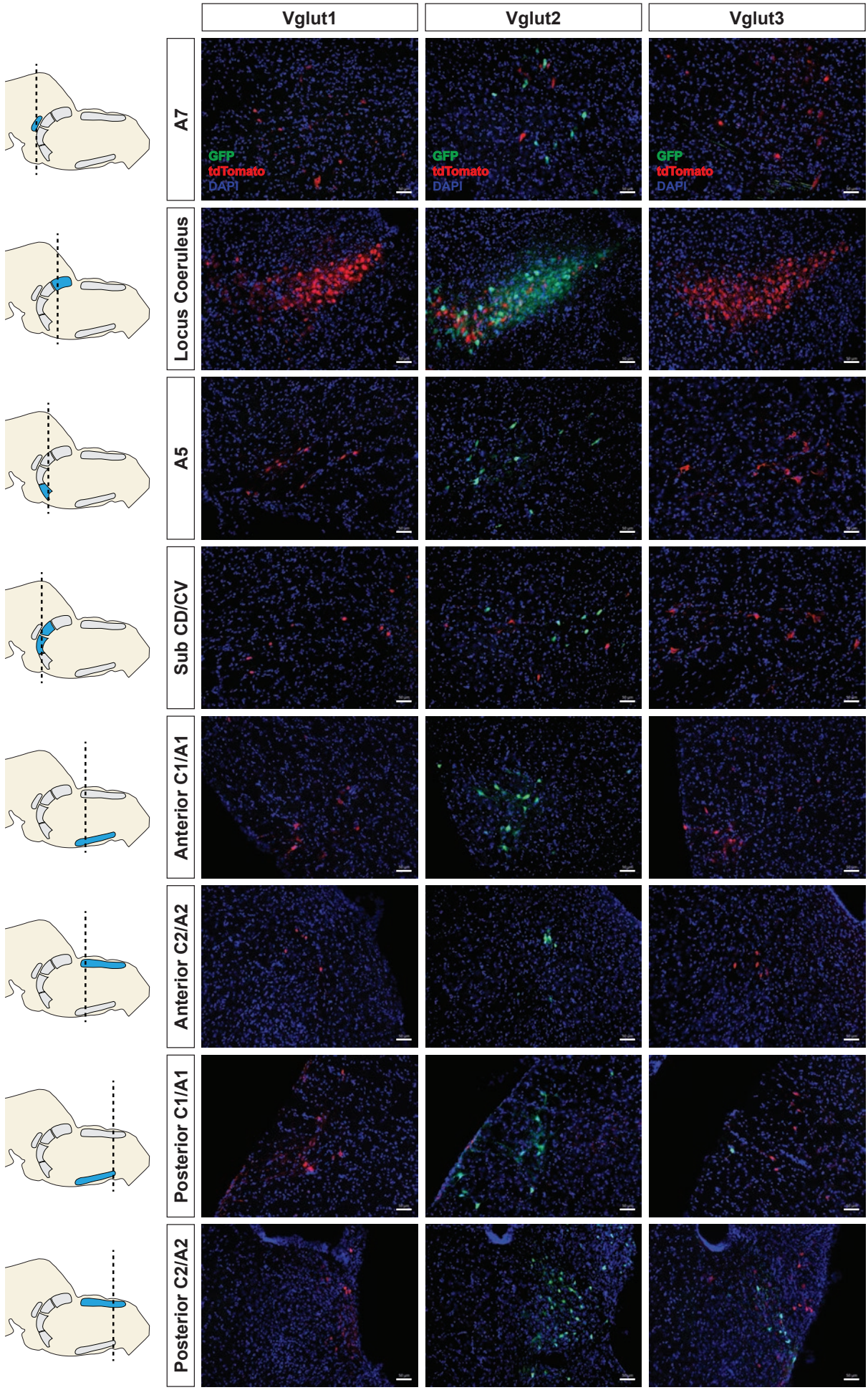

Figure 2

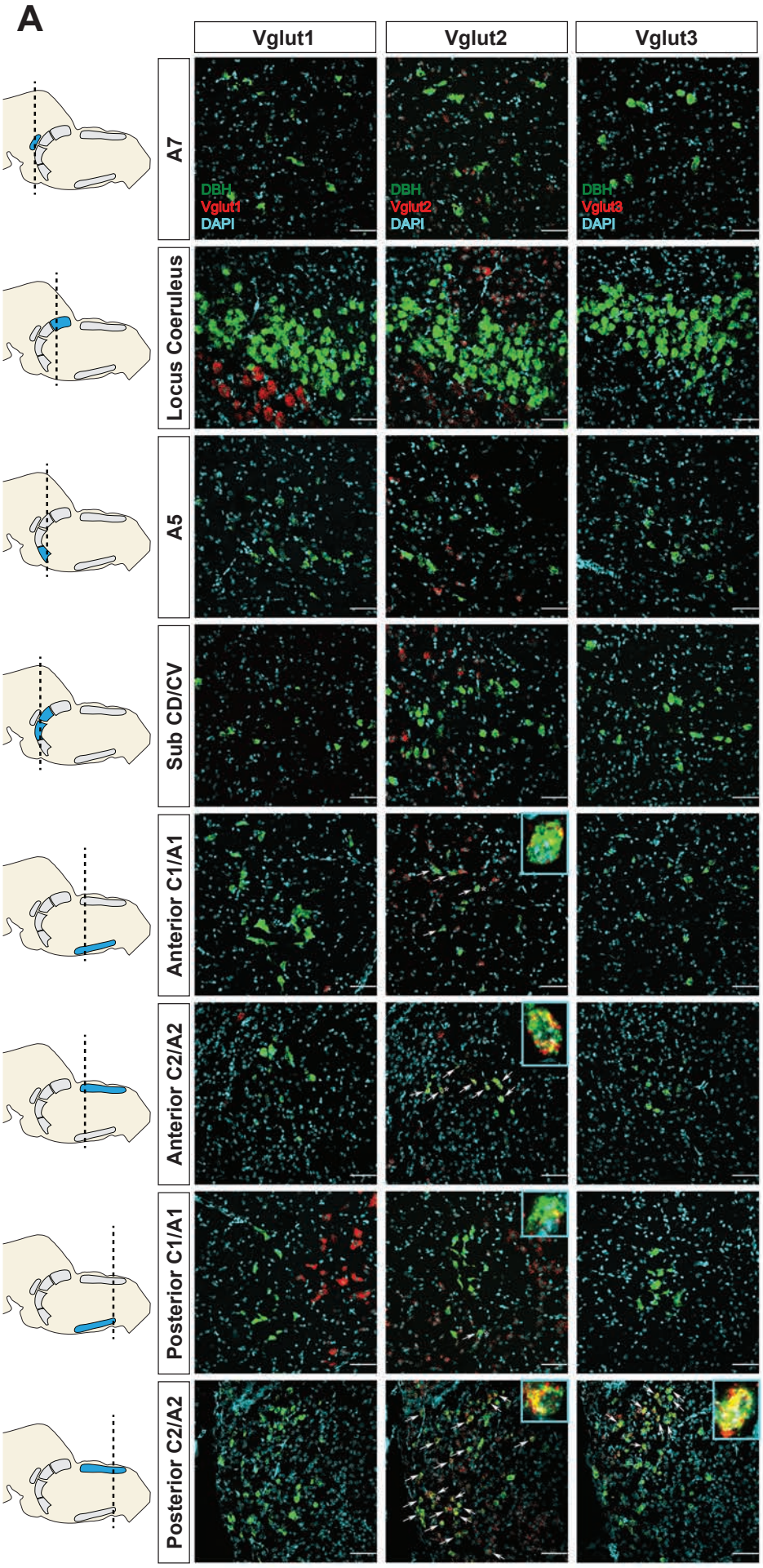
A
Vglut1
Vglut2
Vglut3
A7
Locus Coeruleus
A5
Sub CD/CV
Anterior C1/A1
Anterior C2/A2
Posterior C1/A1
Posterior C2/A2
DBH
Vglut1
DAPI
DBH
Vglut2
DAPI
DBH
Vglut3
DAPI

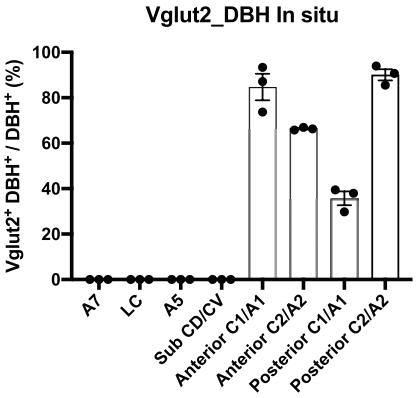
B
Vglut2_DBH In situ
Vglut2+ DBH+ / DBH+ (%)
100
80
60
40
20
0
A7
LC
A5
Sub CD/CV
Anterior C1/A1
Anterior C2/A2
Posterior C1/A1
Posterior C2/A2

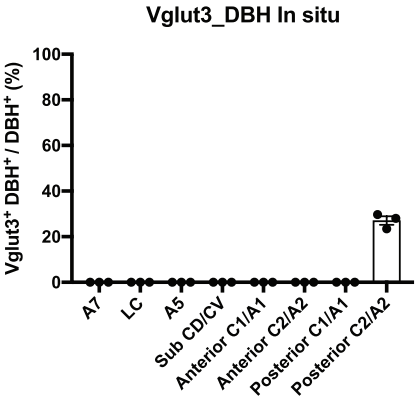
C
Vglut3_DBH In situ
Vglut3+ DBH+ / DBH+ (%)
100
80
60
40
20
0
A7
LC
A5
Sub CD/CV
Anterior C1/A1
Anterior C2/A2
Posterior C1/A1
Posterior C2/A2

Figure 3

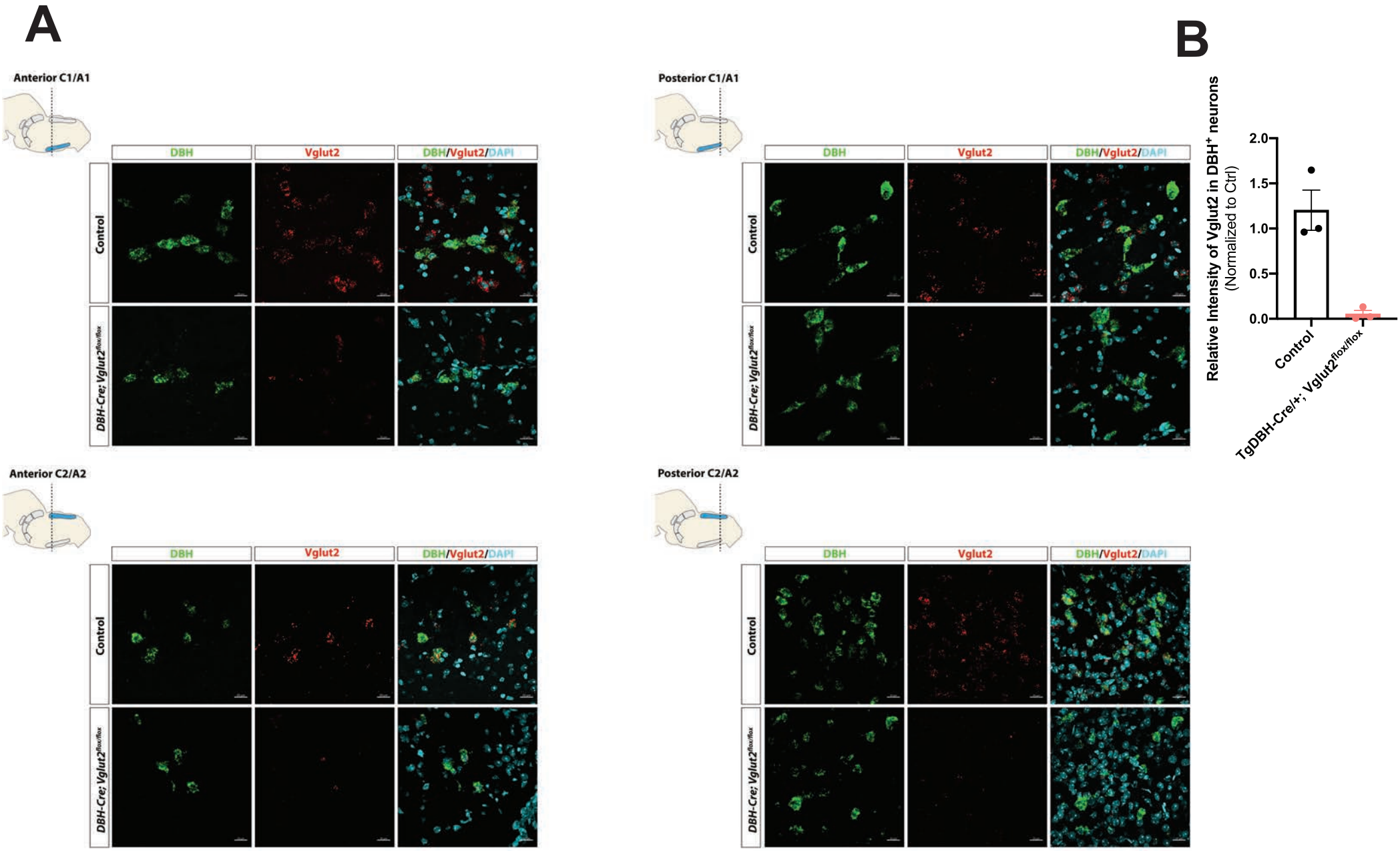
A
Anterior C1/A1
Posterior C1/A1
Anterior C2/A2
Posterior C2/A2
DBH
Vglut2
DBH/Vglut2/DAPI
Control
DBH-Cre; Vglut2flox/flox
B
Relative Intensity of Vglut2 in DBH+ neurons
(Normalized to Ctrl)
2.0
1.5
1.0
0.5
0.0
Control
TgDBH-Cre/+; Vglut2flox/flox

Figure 4

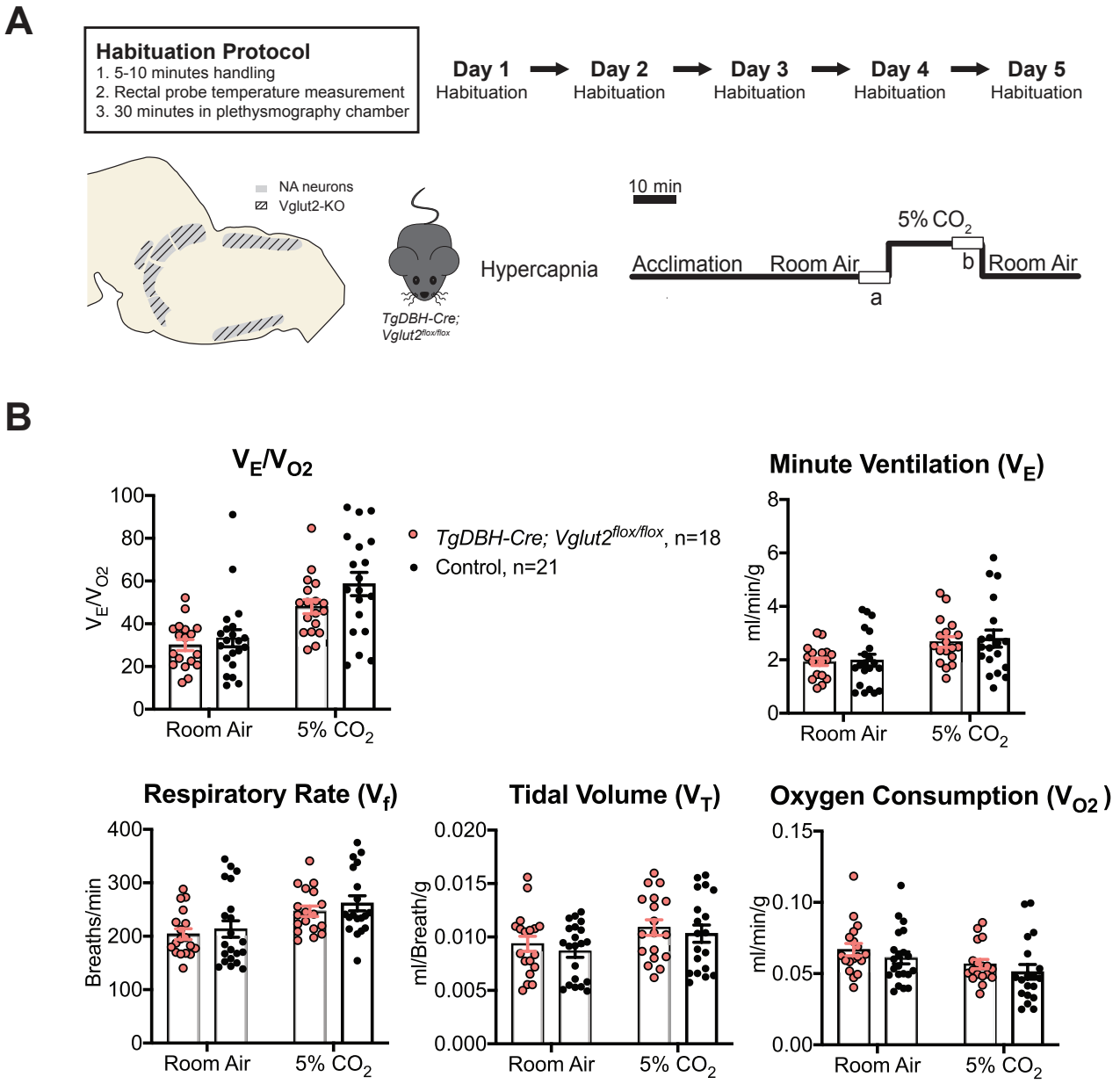
A
Habituation Protocol
1. 5-10 minutes handling
2. Rectal probe temperature measurement
3. 30 minutes in plethysmography chamber
Day 1 Habituation
Day 2 Habituation
Day 3 Habituation
Day 4 Habituation
Day 5 Habituation
NA neurons
Vglut2-KO
TgDBH-Cre; Vglut2flox/flox
Hypercapnia
10 min
5% CO2
Acclimation
Room Air
a
b
Room Air
B
VE/VO2
TgDBH-Cre; Vglut2flox/flox, n=18
Control, n=21
Minute Ventilation (VE)
ml/min/g
Respiratory Rate (Vf)
Breaths/min
Tidal Volume (VT)
ml/Breath/g
Oxygen Consumption (VO2)
ml/min/g
Room Air
5% CO2

Figure 5

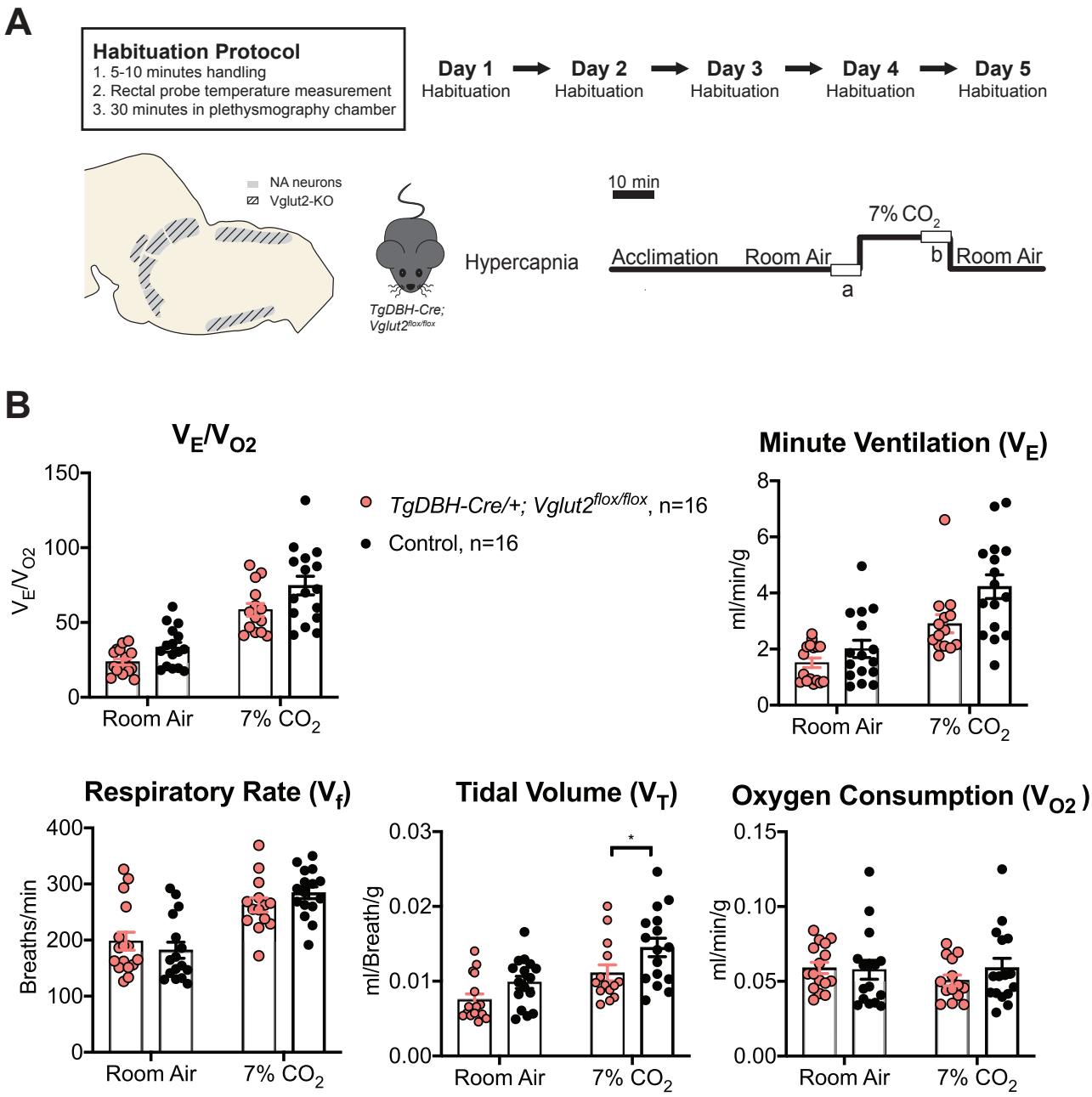
A
Habituation Protocol
1. 5-10 minutes handling
2. Rectal probe temperature measurement
3. 30 minutes in plethysmography chamber
Day 1 Habituation
Day 2 Habituation
Day 3 Habituation
Day 4 Habituation
Day 5 Habituation
NA neurons
Vglut2-KO
TgDBH-Cre; Vglut2flox/flox
Hypercapnia
10 min
Acclimation
Room Air
7% CO2
a
b
Room Air
B
VE/VO2
TgDBH-Cre/+; Vglut2flox/flox, n=16
Control, n=16
Room Air
7% CO2
Minute Ventilation (VE)
ml/min/g
Respiratory Rate (Vf)
Breaths/min
Tidal Volume (VT)
ml/Breath/g
*
Oxygen Consumption (VO2)
ml/min/g

Figure 6

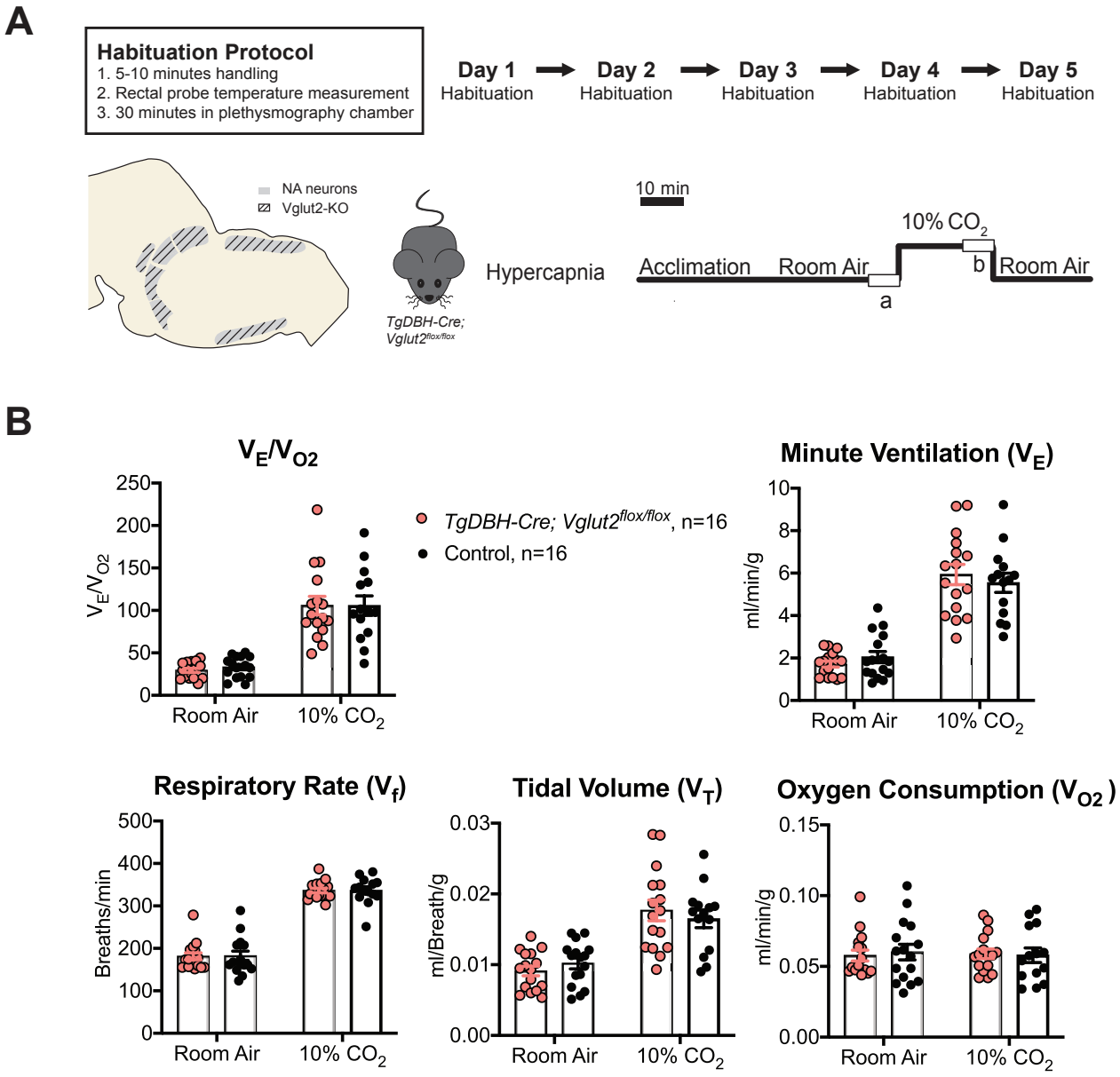
A
Habituation Protocol
1. 5-10 minutes handling
2. Rectal probe temperature measurement
3. 30 minutes in plethysmography chamber
Day 1 Habituation
Day 2 Habituation
Day 3 Habituation
Day 4 Habituation
Day 5 Habituation
NA neurons
Vglut2-KO
TgDBH-Cre; Vglut2flox/flox
Hypercapnia
10 min
10% CO2
Acclimation
Room Air
a
b
Room Air
B
VE/VO2
TgDBH-Cre; Vglut2flox/flox, n=16
Control, n=16
Minute Ventilation (VE)
ml/min/g
Respiratory Rate (Vf)
Breaths/min
Tidal Volume (VT)
ml/Breath/g
Oxygen Consumption (VO2)
ml/min/g
Room Air
10% CO2

Figure 7

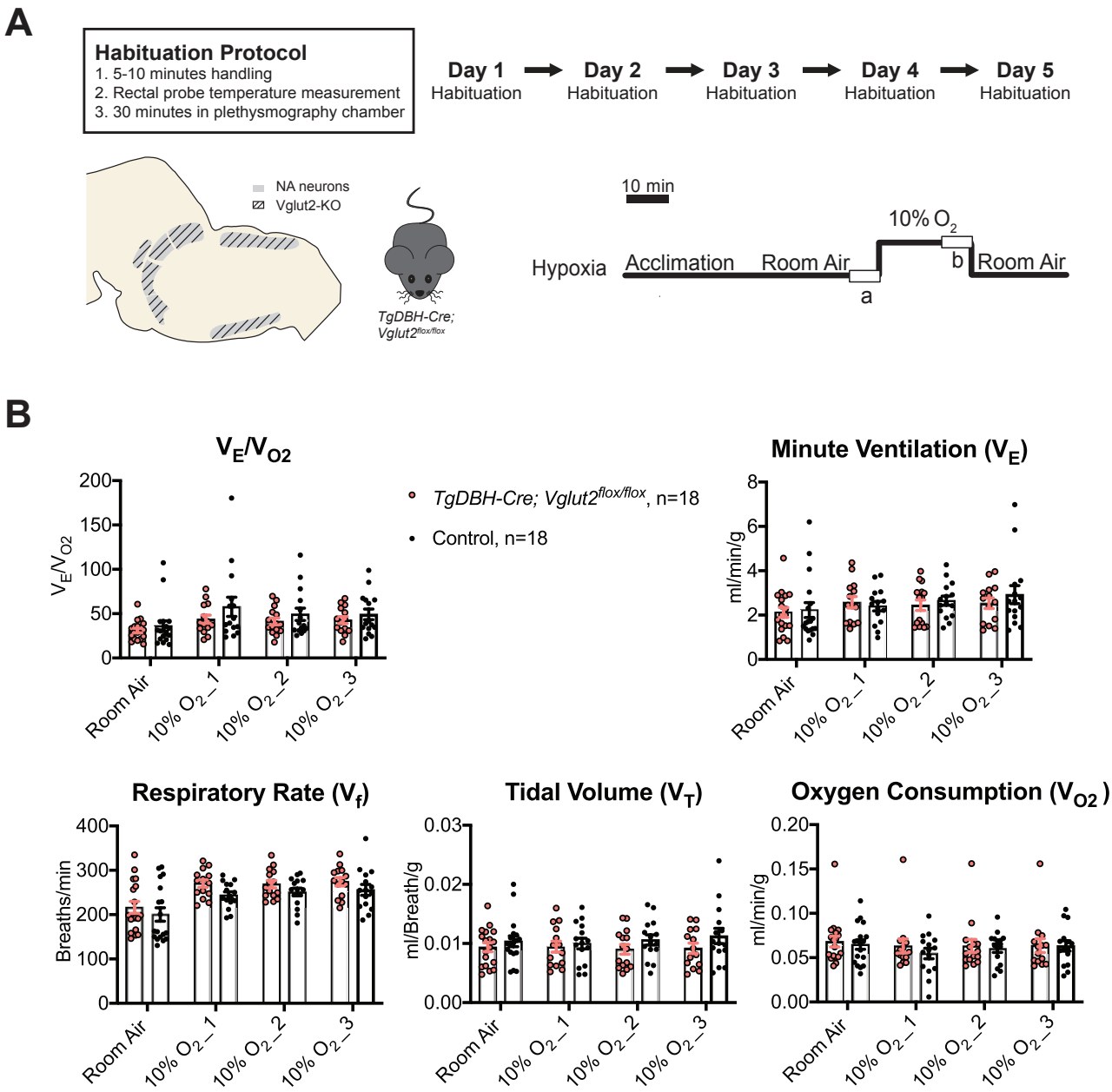
A
Habituation Protocol
1. 5-10 minutes handling
2. Rectal probe temperature measurement
3. 30 minutes in plethysmography chamber
Day 1 Habituation
Day 2 Habituation
Day 3 Habituation
Day 4 Habituation
Day 5 Habituation
NA neurons
Vglut2-KO
TgDBH-Cre; Vglut2flox/flox
10 min
10% O2
Hypoxia
Acclimation
Room Air
a
b
Room Air
B
VE/VO2
TgDBH-Cre; Vglut2flox/flox, n=18
Control, n=18
Minute Ventilation (VE)
ml/min/g
Room Air
10% O2_1
10% O2_2
10% O2_3
Respiratory Rate (Vf)
Breaths/min
Tidal Volume (VT)
ml/Breath/g
Oxygen Consumption (VO2)
ml/min/g

Figure 2 supplement 1

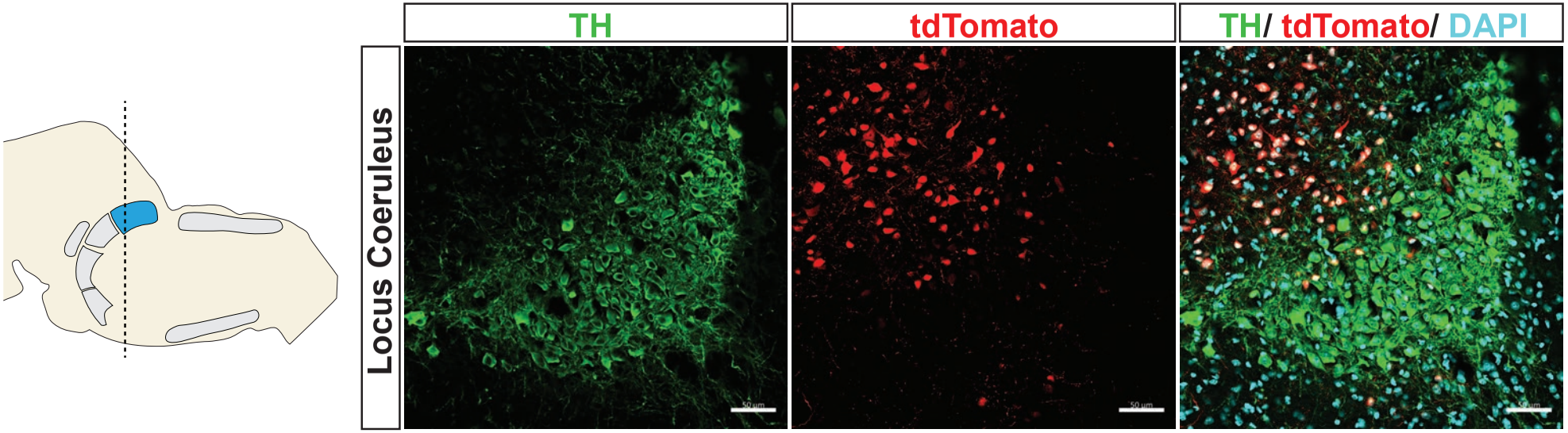

Table 1. Respiratory and metabolic values under room air conditions and the statistical tests

	TgDBH-Cre/+; Vglut2$^{flox/flox}$ **Mean ± SEM**	**Control Mean ± SEM**	***TgDBH-Cre/+; Vglut2$^{flox/flox}$*** **vs Control linear mixed-effects regression model**
V_E/V_{O2}	30.01 ± 2.58	33.22 ± 3.97	P = 0.98
V_f	204.08 ± 10.04	213.58 ± 15.36	P = 0.98
V_T	0.009 ± 0.0007	0.009 ± 0.0006	P = 0.88
V_E	1.93 ± 0.14	1.98 ± 0.22	P = 0.995
V_{O2}	0.067 ± 0.004	0.061 ± 0.004	P = 0.78

Table 2. Respiratory and metabolic values under 5% CO_2 conditions and the statistical tests

	TgDBH-Cre/+; Vglut2$^{flox/flox}$ **Mean ± SEM**	**Control Mean ± SEM**	***TgDBH-Cre/+; Vglut2$^{flox/flox}$*** **vs Control linear mixed-effects regression model**
V_E/V_{O2}	47.99 ± 3.28	58.60 ± 5.44	P = 0.33
V_f	246.72 ± 9.78	261.66 ± 14.00	P = 0.24
V_T	0.011 ± 0.0007	0.010 ± 0.0008	P = 0.81
V_E	2.67 ± 0.20	2.80 ± 0.32	P = 0.98
V_{O2}	0.057 ± 0.003	0.051 ± 0.005	P = 0.42

Table 3. Respiratory and metabolic values under 7% CO_2 conditions and the statistical tests

	TgDBH-Cre/+; Vglut2$^{flox/flox}$ **Mean ± SEM**	**Control Mean ± SEM**	***TgDBH-Cre/+; Vglut2$^{flox/flox}$*** **vs Control linear mixed-effects regression model**
V_E/V_{O2}	58.48 ± 4.29	74.70 ± 6.22	P = 0.23
V_f	262.69 ± 12.82	284.44 ± 10.59	P = 0.98
V_T	0.011 ± 0.0011	0.015 ± 0.0012	P = 0.023*
V_E	2.90 ± 0.32	4.23 ± 0.43	P = 0.16
V_{O2}	0.051 ± 0.004	0.059 ± 0.006	P = 0.64

Table 4. Respiratory and metabolic values under 10% CO_2 conditions and the statistical tests

	TgDBH-Cre/+; Vglut2$^{flox/flox}$ **Mean ± SEM**	**Control Mean ± SEM**	***TgDBH-Cre/+; Vglut2$^{flox/flox}$*** **vs Control linear mixed-effects regression model**
V_E/V_{O2}	105.77 ± 10.80	105.69 ± 11.51	P = 0.9996
V_f	336.31 ± 5.26	336.38 ± 8.52	P = 0.9997
V_T	0.018 ± 0.0015	0.016 ± 0.0012	P = 0.98
V_E	5.94 ± 0.48	5.54 ± 0.45	P = 0.9996
V_{O2}	0.059 ± 0.003	0.058 ± 0.005	P = 0.9999999

Table 5. Respiratory and metabolic values under 10% O_2 conditions and the statistical tests

	TgDBH-Cre/+; Vglut2$^{flox/flox}$ **Mean ± SEM**	**Control Mean ± SEM**	**Linear mixed-effects regression model**	***TgDBH-Cre/+; Vglut2$^{flox/flox}$*** **Mean ± SEM**	**Control Mean ± SEM**	**Linear mixed-effects regression model**	***TgDBH-Cre/+; Vglut2$^{flox/flox}$*** **Mean ± SEM**	**Control Mean ± SEM**	**Linear mixed-effects regression model**
	10% O_2_1			**10% O_2_2**			**10% O_2_3**		
V_E/V_{O2}	43.79 ± 4.57	57.75 ± 10.88	P = 0.99	41.30 ± 3.85	49.36 ± 6.93	P = 0.99	42.82 ± 3.97	49.19 ± 6.02	P = 0.99
V_f	269.71 ± 8.49	243.89 ± 7.64	P = 0.67	268.38 ± 8.40	251.15 ± 8.67	P = 0.83	273.96 ± 9.31	255.84 ± 12.19	P = 0.80
V_T	0.009 ± 0.0009	0.010 ± 0.0009	P = 0.89	0.009 ± 0.0008	0.011 ± 0.0009	P = 0.85	0.009 ± 0.0009	0.011 ± 0.0013	P = 0.64
V_E	2.58 ± 0.25	2.40 ± 0.21	P = 0.999998	2.45 ± 0.24	2.65 ± 0.21	P = 0.9998	2.53 ± 0.24	2.92 ± 0.41	P = 0.998
V_{O2}	0.063 ± 0.008	0.055 ± 0.006	P = 0.995	0.063 ± 0.007	0.061 ± 0.005	P = 0.9998	0.064 ± 0.008	0.063 ± 0.006	P = 0.99999999